



Originally published as:

Dietze, E., Slowinski, M., Zawiska, I., Veh, G., Brauer, A. (2016): Multiple drivers of Holocene lake level changes at a lowland lake in northeastern Germany. - *Boreas*, 45, 4, pp. 828–845.

DOI: <http://doi.org/10.1111/bor.12190>

# 1 **Multiple drivers of Holocene lake level changes at a lowland lake in northeastern Germany**

2 ELISABETH DIETZE, MICHAŁ SŁOWIŃSKI, IZABELA ZAWISKA, GEORG VEH AND ACHIM BRAUER

3

4 Dietze, E., Słowiński, M., Zawiska, I., Veh, G., Brauer, A.: Multiple drivers of Holocene lake

5 level changes at a lowland lake in northeastern Germany

6

7 Many German lakes experienced significant water level declines in the last decades that are  
8 not fully understood due to the short observation period. At a typical northeastern German  
9 groundwater-fed lake with complex basin morphology, an acoustic sub-bottom profile was  
10 analysed together with a transect of five sediment cores, which were correlated using multiple  
11 proxies (sediment facies,  $\mu$ -XRF, macrofossils, subfossil *Cladocera*). Shifts in the boundary  
12 between sand and mud deposition were controlled by lake level changes, and hence, allowed  
13 the quantification of an absolute lake level amplitude of ~8 m for the Holocene. This clearly  
14 exceeded observed modern fluctuations of 1.3 m (AD1973-2010). Past lake level changes were  
15 traced continuously using the Calcium-record. During high lake levels, massive organic muds  
16 were deposited in the deepest lake basin, whereas lower lake levels isolated the sub-basins  
17 and allowed carbonate deposition.

18 During the beginning of the Holocene (>9700 cal. a BP), lake levels were high likely due to final  
19 melting of permafrost and dead-ice remains. The establishment of water use intensive *Pinus*  
20 forests caused generally low (3-4 m below modern) but fluctuating lake levels (9700-6400 cal.  
21 a BP). Afterwards, the lake showed an increasing trend and reached a short-term high-stand  
22 ~5000 cal. a BP (4 m above modern). At the transition towards a cooler and wetter late  
23 Holocene, forests dominated by *Quercus* and *Fagus* and initial human impact likely  
24 contributed more positively to groundwater recharge. Lake levels remained high between  
25 3800 and 800 cal. a BP, but the lake system was not sensitive enough to record short-term  
26 fluctuations during this period. Lake level changes were recorded again, when humans  
27 profoundly affected the drainage system, land cover and lake trophy. Hence, local Holocene  
28 water level changes reflect feedbacks between catchment and vegetation characteristics and  
29 human impact superimposed by climate change at multiple temporal scales.

30

31

32 Elisabeth Dietze (edietze@gfz-potsdam.de), Michał Słowiński, Izabela Zawiska and Achim  
33 Brauer, Section 5.2 Climate Dynamics and Landscape Evolution, GFZ German Research  
34 Centre for Geosciences, Potsdam 14473, Germany; Michał Słowiński, Department of  
35 Environmental Resources and Geohazards, Institute of Geography and Spatial Organization,  
36 Polish Academy of Sciences, Kopernika 19, Toru\_n PL-87-100, Poland; Izabela Zawiska,  
37 Department of Geoecology and Climatology, Institute of Geography and Spatial  
38 Organization, Polish Academy of Sciences, Twarda 51/55, Warsaw PL-00-818, Poland; Georg  
39 Veh, Chair of Physical Geography, Catholic University of 2 Eichstaett-Ingolstadt, Ostenstraße  
40 14, Eichstaett 85072, Germany; Georg Veh, Institute for Earth and Environmental Sciences,  
41 University of Potsdam, Karl-Liebnecht-Straße 24-25, Potsdam 14476, Germany; received  
42 16th December 3 2015, accepted 4th May 2016.

43

44 The hydrological system is a vulnerable landscape component showing considerable variability  
45 in different areas of the world (Allen & Ingram 2002; Gronewold & Stow 2014), which  
46 complicates predictions in the context of future climate change (Sherwood & Fu 2014). During  
47 the last 30 to 50 years, groundwater-fed lakes in northeastern Germany showed a significant  
48 lowering (Germer *et al.* 2011; Kaiser *et al.* 2014a), which was linked to decreasing water  
49 availability in response to global climate change (Natkhin *et al.* 2012). However, lake levels  
50 have started to rise again since ~AD2008, in contrast to predictions (Natkhin *et al.* 2012). This  
51 unexpected development revealed our incomplete understanding regarding regional  
52 hydrological responses to global environmental changes, calling for additional  
53 palaeohydrological studies.

54         Depending on the natural configuration of a landscape, different archives provide  
55 proxy information on components of past water cycles; for example, lakes provide lake level  
56 proxies indicating palaeo-water balances. Morphological-sedimentological features within  
57 lake basins provide discrete but absolute lake level reconstructions (Dietze *et al.* 2010, 2013).  
58 Continuous reconstructions from profundal lake sediment cores use relationships  
59 between water depth and certain biological proxies (Hannon and Gaillard, 1997; Korhola *et al.*  
60 2000; Laird *et al.* 2011). Also authigenic carbonate has been used as a relative lake level proxy  
61 (Haberzettl *et al.* 2005; Pompeani *et al.* 2012).

62         Multiple cores collected along transects from littoral to profundal sites enable the  
63 reconstruction of lake level changes (Digerfeldt 1986; Magny 2004; Pribyl & Shuman 2014). In  
64 the European Alps, high detrital carbonate input into lakes has allowed absolute and highly-  
65 resolved lake level reconstructions using changes in precipitated carbonate morphologies  
66 related to water depth (Magny 2004). In temperate humid areas with low detrital carbonate  
67 input, complementary biological and sedimentological proxies have been related to lake level  
68 changes, e.g. macrofossils and the position of the sediment limit, i.e., the upper limit for the  
69 predominant deposition of organic-rich mud related to sediment focusing (Digerfeldt 1986;  
70 Dearing 1997). The “Digerfeldt approach” has provided reliable lake level reconstructions  
71 across the globe (e.g. Punning *et al.* 2004; Shuman *et al.* 2010; Haig *et al.* 2013), but so far has  
72 been restricted to shallow lakes <100 ha with simple basin morphologies (e.g. low-angled  
73 slopes <4%; Digerfeldt 1986; Pribyl & Shuman 2014).

74 In the central European lowlands, hydrological reconstructions primarily rely on records from  
75 small lakes or peat bogs (Gałka *et al.* 2013, 2014; Słowiński *et al.* 2015). In northeastern

76 Germany, a high sensitivity of lakes to Holocene hydrological changes has been suggested (e.g.  
77 Lampe *et al.* 2009; Kaiser *et al.* 2012, 2014b; Küster *et al.* 2014); however, well-dated lake  
78 level reconstructions remained restricted to certain times.

79 Lake Fürstenseer See, a typical groundwater fed lake with complex morphology has  
80 already showed pronounced changes in lake level and size during the instrumental period  
81 (Germer *et al.* 2011; Kaiser *et al.* 2014a), suggesting that its sediments may provide a highly  
82 sensitive record of past hydrological shifts. The first acoustic sub-bottom profile of  
83 northeastern German lakes was analysed together with a transect of five sediment cores  
84 across the deepest sub-basin to evaluate the potential of different sedimentological and  
85 biological proxies to reconstruct Holocene lake level changes in such a setting. The main aims  
86 of this study are to reconstruct i) full Holocene water level amplitudes, ii) the Holocene lake  
87 level history and iii) to discuss potential driving mechanisms that caused these past lake level  
88 changes.

89

#### 90 Study area

91 Lake Fürstenseer See (53°19' N, 13°12' E, ~63 m a.s.l., Fig. 1) formed after the retreat of the  
92 Weichselian ice sheet in the direct forefront of the Pommerian ice margin ( $W2_{max}$ , 18-20 ka,  
93 Lüthgens & Böse, 2011; Fig. 1A). This outwash plain area is characterized by sandy and gravelly  
94 glaciofluvial sediments (<1-2% silt and clay). Today, *Fagus* and *Pinus* forests dominate the 33.4  
95 km<sup>2</sup> catchment (63%) followed by 18% agricultural land, lakes (13%), peatlands (5%), and  
96 settlements (1%, Kaiser *et al.* 2014a). Within the sub-maritime to sub-continental temperate  
97 humid climate zone, Neustrelitz (~5 km west of the lake) has a mean annual temperature  
98 (precipitation) of 8.0 °C (584 mm) with most precipitation occurring as summer rainfall (range:  
99 428-814 mm, 1961-1990, Stüve 2010). Main wind directions are from the west (P. Stüve, pers.  
100 comm. 2014).

101 There are no surficial inflows to this naturally closed lake system suggesting  
102 groundwater as the primary source of recharge to the lake. This is supported by monthly lake  
103 level variability in the period AD1973-2010 co-varied with groundwater recharge (Stüve 2010;  
104 Fig. 1D). However, since at least the 17th century and until the establishment of the Müritz  
105 national park in AD199, the lake was artificially connected to adjacent lakes (Kaiser *et al.*  
106 2014b). Kaiser *et al.* (2014b) reconstructed a 3 m higher lake stand during the late Medieval  
107 time, but full water level amplitudes are unknown for the Holocene.

108 In September 2011 (water level: 63.71 m a.s.l.), the ~240 ha large dimictic lake had a  
109 volume of 17.4 Mio. m<sup>3</sup>, a perimeter of 19.9 km, a maximum water depth (w.d.) of 25 m ( $z_{\text{mean}}$   
110 = 6.9 m) and a catchment to lake ratio of 14:1. In the deepest, i.e., south-eastern sub-basin  
111 (Fig. 1B), discontinuous water quality observations revealed Secchi depths at  $5.2 \pm 1.2$  m w.d.,  
112 pH of  $8 \pm 0.6$  and electrical conductivity of  $262 \pm 23$  mS cm<sup>-1</sup>. The thermocline was established  
113 at ~10 m w.d. in summers (1973-2011, Ministerium für Landwirtschaft, Umwelt und  
114 Verbraucherschutz Mecklenburg-Vorpommern, pers. comm. 2012). Modern macrophyte  
115 surveys have revealed a high water plant diversity dominated by *Chara spec.* (Kirschey &  
116 Oldorff 2012).

117

## 118 **Material and methods**

### 119 *Field methods*

120 For estimations of present and past lake areas and volumes, bathymetric survey points from  
121 October 2002 (Ministerium für Landwirtschaft, Umwelt und Verbraucherschutz Mecklenburg  
122 Vorpommern, pers. comm. 2013) were interpolated using triangulation (SAGA-GIS 2.2)  
123 supported by near-shore elevations from an airborne laser scanning digital elevation model (1  
124 m horizontal, 0.2 m vertical resolution; Amt für Geoinformation, Vermessungs- und  
125 Katasterwesen Mecklenburg-Vorpommern, pers. comm. 2013).

126 To detect the modern mud-sand boundary (i.e. modern sediment limit), an acoustic sub-  
127 bottom profile across the southeastern bay was performed in May 2014 using a SES-96  
128 sediment echo sounder from Innomar Technologie GmbH (frequency 10 kHz, gain 14 dB,  
129 sound velocity 1462 m s<sup>-1</sup>). In the same bay, five lake sediment cores along a 173 m long  
130 transect between 10 and 23 m w.d. were recovered in October 2008 (short core GFS10-8) and  
131 in September 2011 (four long cores GFS11; Fig. 1B, C, Tab. 1). An Uwitec piston corer  
132 recovered 2-m long drives from one borehole at each site, with an overlapping additional short  
133 core next to the long drives. All relative water depths mentioned below refer to an absolute  
134 level of 63.71 m a.s.l. (September 2011). Cores were split and macroscopically described after  
135 Schnurrenberger *et al.* (2003). Sediments from cores GFS11-AB, -C and -E were microscopically  
136 inspected using smear slides and thin sections (preparation after Brauer & Casanova 2001).

137

### 138 *Geochemical analyses*

139 The sediment composition of the long cores was continuously analysed with an ITRAX  $\mu$ -X-ray  
140 fluorescence ( $\mu$ -XRF) core scanner (Cr-HE-tube, 40 kV, 40 mA, 1 mm step size, 500 ms exposure  
141 time). Nine elements (Si, S, K, Ca, Ti, Fe, Rb, Sr, Zr) with less than 5% zero values were used  
142 further. Element intensities from XRF core scanning are influenced by down core changes of  
143 physical properties, the sample geometry, enhancement and absorption effects (Tjallingii *et*  
144 *al.* 2007). They are non-linear functions of geochemical concentrations, whereas log-ratios of  
145 element intensities are linearly related to log-ratios of concentrations (Weltje & Tjallingii  
146 2008). Hence, element intensities were transformed with a centered log-ratio (clr) using the  
147 R-package “robCompositions” (Templ *et al.* 2011) to prevent mis-interpretations, which are  
148 further related to the compositional nature of geochemical data.

149 Composite core stratigraphies were derived from overlapping cores using  
150 macroscopically visible boundaries and the Ca record. To derive objective boundaries for the  
151 lithological units of the composite cores GFS11-C, -D and -E, a depth-constrained hierarchical  
152 cluster analysis (CONISS, Grimm 1987) was performed using the clr-transformed element data  
153 and the ratio of incoherent and coherent scattering ( $Cr_{inc}/Cr_{coh}$ , representing elements lighter  
154 than Al) in the R-package “rioja” (Juggings 2012).

155 Discrete samples were taken from blackish, greyish and whitish stratigraphic layers to  
156 measure total nitrogen (TN) and total carbon (TC) with an elemental analyser (EA3000-CHNS  
157 Eurovector). Samples with a volume of one  $cm^3$  ( $n = 195$ ; see Fig. S1 for sample positions) were  
158 freeze-dried, milled and prepared as 5 mg aliquots in Sn capsules. Additional 3 mg aliquots  
159 were decalcified in Ag capsules with 20% HCl and dried at 85 °C to measure total organic  
160 carbon (TOC). The analytical precision is 0.01%. C/N ratios and amount of carbonate (TIC)  
161 could then be calculated.

162

### 163 *Biological analyses*

164 Discrete samples from the main lithological units were analysed for macrofossil remains ( $n =$   
165 71) and subfossil *Cladocera* composition ( $n = 39$ , Fig. S1). Macrofossil samples were washed  
166 on 125  $\mu m$  sieves and analysed according to Birks (2007). All macrofossil counts were  
167 standardised as numbers of fossils per 50  $cm^3$ . Determination of macrofossil remains was  
168 based on the literature (Birks 2007; Tobolski 2000; Velichkevich & Zastawniak 2006, 2008) and  
169 a reference collection of the Institute of Geography, Polish Academy of Science.

170 *Cladocera* samples were heated, stirred 20 minutes in a 10% solution of KOH and washed  
171 through a 38- $\mu$ m sieve following Frey (1986). Samples were then analysed using a transmitted-  
172 light microscope at magnifications of 100x to 400x. All counted *Cladocera* remains  
173 (headshields, shells, ehippia, postabdomens) and the most abundant body part of each  
174 species were considered to represent the number of individuals. A minimum of 200 individuals  
175 per sample were identified based on Szeroczyńska & Sarmaja-Korjonen (2007). Subfossil  
176 *Cladocera* data was evaluated using a detrended correspondence analysis (DCA) after Hill &  
177 Gauch (1980) in the R-package “vegan” (Oksanen *et al.* 2013). The first two axes had axis  
178 lengths >1.3 and were chosen to represent the dataset.

179

### 180 *Dating and core correlation*

181 AMS <sup>14</sup>C dating was performed on 22 samples of terrestrial plant remains at Poznań  
182 Radiocarbon Laboratory (Tab. 2). Calibration was done using Oxcal 4.2 (Bronk Ramsey 2008)  
183 and the IntCal13 dataset (Reimer *et al.* 2013). Age-depth modelling was performed for the  
184 longest continuous core GFS11-D. A Bayesian p-sequence depositional age-depth model was  
185 calculated with Oxcal 4.2 using a k-value of 1 cm and allowing sedimentation rate to vary  
186 within U(-1,1). This was a rather limited range of freedom, in contrast to the suggestion by  
187 Bronk Ramsey & Lee (2013) to use U(-2,2), which introduced unrealistic sedimentation rates  
188 (not shown). Sediment cores were correlated using sediment facies and multi-proxy analyses.

189

## 190 **Results**

### 191 *Basin morphology and acoustic transect*

192 The bathymetric survey revealed that the lake basin of Lake Fürstenseer See has a complex  
193 morphology (shoreline development = 5.5, Hutchinson 1957; Fig. 1A). The two main elongated  
194 basins follow the general paraglacial meltwater flow direction from northeast to southwest.  
195 These basins contain several sub-basins and are linked by a shallow area that falls dry in times  
196 of instrumentally recorded low lake stands. The steepest slopes occur along the eastern shores  
197 and southeastern sub-basin. In the southeastern sub-basin, which is the deepest (Fig. 1B, C),  
198 the maximum fetch along the prevailing wind direction is up to 1 km (Tab. 1) leading to strong  
199 turbulence in the upper water column. During the time period 1973 to 2013 (Fig. 1D) the lake  
200 level, area and volume changed interannually by ~2.1% (i.e., 1.3 m), 49% and 23%,  
201 respectively.



202 Sediment cores were located in the southeastern sub-basin, between 81 to 191 m from  
203 the shore (GFS11-AB to -E, respectively). Slopes were steepest at site GFS11-AB (22.5%) and  
204 shallowest at the deepest site (2.4% at GFS11-E, Tab. 1). Across the core transect, an acoustic  
205 sub-bottom profile indicated a clear mud-sand boundary at ~14 m w.d., i.e. the modern  
206 sediment limit (Fig. 3). At this depth, the first reflector at the sediment-water interface  
207 changed from very high backscatter representative of dense, sandy sediments upslope  
208 towards very low, almost transparent impedance contrasts of onlapping reflections that  
209 represent fine-grained, water-saturated mud from calm pelagic deposition below the storm  
210 wave base. Sediment focusing caused increasing sediment thickness below 14 m w.d.  
211 However, the deepest part of the sub-basin was masked by gas, as is typical in such  
212 environments (Gilbert 2003; i.e., diffuse reflections directly at the sediment-water interface  
213 and high scattering of the acoustic waves within the water column, Fig. 3).

214

#### 215 *Sediment facies, geochemical and biological results*

216 Along the core transect, different lithological units (LU) were distinguished by visual  
217 descriptions after Schnurrenberger *et al.* (2003; all cores) and CONISS-clustering of the  $\mu$ -XRF-  
218 data (mud-dominated cores GFS11-C, -D, -E; Tab. 2). LU were numbered from top to bottom  
219 for each core separately. Sand layers and distinct LU-boundaries indicated unconformities.  
220 Continuity of sedimentation increased with water depth (Figs 3, S1).

221 Three main sediment facies were distinguished across the transect: sands, blackish  
222 organic muds, and greyish carbonate muds. The 1.9 m long core GFS11-AB at 10 m w.d.  
223 primarily consisted of fine to coarse, partly bedded sands with organic detritus and some  
224 gravel, except for LU2. This 9 cm thick layer of fine-grained carbonate-rich mud contained 5-  
225 10  $\mu$ m long calcite crystals accumulated with up to 30  $\mu$ m diameter *Chara spec.* oogonia and  
226 thin amorphous organic matter layers (no sand, Fig. S2). At 15.2 m w.d., core GFS11-C  
227 contained 3.7 m of dominantly fine-grained, organic- and carbonate-rich muds intercalated  
228 with several sand layers in a carbonate mud matrix at 210 to 280 cm sediment depth (LU5).  
229 Two fining-upwards sand layers at 165 to 178 cm sediment depth (LU4) may have resulted  
230 from erosional events upslope. At 19.8 m w.d., the 8.4 m long core GFS11-D was completely  
231 composed of alternating blackish organic mud and greyish calcareous mud sequences and did  
232 not contain any sand layers. The 6.3 m long core GFS11-E at 23 m w.d. had similar, but slightly

233 thicker, lithological units to core GFS11-D. In contrast to cores GFS11-AB and -C, cores GFS11-  
234 D and -E did not reach the lacustrine sediment base.

235 Organic muds consisted of decomposed organic matter (sometimes identifiable as  
236 aquatic plant remains), varying contents of diatoms, chrysophytes, secondary pyrite and few  
237 dispersed sand-sized mineral grains (Fig. S2). Carbonate muds differed from organic muds by  
238 the additional appearance of micritic calcite in cores GFS11-C to -E. Finer crystals than the  
239 littoral calcites of GFS11-AB-LU2 (Fig. S2) suggest dominantly pelagic carbonate precipitation.  
240 Dry densities were  $0.24 \pm 0.2$  and  $0.81 \pm 0.4$  g cm<sup>-3</sup> for mud and sand facies, respectively.

241 TOC contents were generally very high ( $15 \pm 9\%$ ,  $n = 195$ ) and C/N was between 10 and  
242 20, but close to 10 in all mud units independent of carbonate content (Fig. S1, Tab. S1),  
243 revealing the dominance of authigenic organic matter production (Meyers & Ishiwatari 1993)  
244 with terrestrial matter input contributing primarily to sand layers.

245 The main lithological variation between blackish organic and greyish carbonate muds  
246 can be illustrated by the continuous Ca record as a proxy for authigenic carbonate  
247 preservation (i.e. high Ca in carbonate muds, Fig. S1; no detrital calcite found in microscopic  
248 inspection, Fig. S2). Clr-transformed Ca was positively correlated with TIC ( $r = 0.76$ ). Ca was  
249 negatively correlated with most other elements (e.g. Ti, K, Fe; not shown).

250 Macrofossil analyses revealed a strong presence of *Chara spec. oogonia*, but other water  
251 and wetland plant remains occurred only marginally in few samples. Subfossil *Cladocera*  
252 analyses indicated relatively similar species compositions through time, dominated by the  
253 open-water turbidity-tolerating species *Bosmina longirostris* (Bjerring *et al.* 2009), the  
254 eutrophy-tolerant species *Chydorus sphaericus* (Vijverberg & Boersma 1997) and varying  
255 amounts of a few further pelagic and littoral species (Fig. S1, Tab. S2).

256

### 257 *Core correlation*

258 Stratigraphic correlation of sediment facies and LU between the cores was supported by  
259 sedimentological and subfossil *Cladocera* analyses (Fig. 3). The topmost units LU1 to 3 in cores  
260 GFS11-C to -E and LU1/2 in core GFS10-8 had similar facies and subfossil *Cladocera*  
261 compositions (Fig. S1). However, the thicknesses of LU1 to 3 increased with water depth due  
262 to sediment focusing, allowing the subdivision of LU2 in the two deepest cores (Fig. 3). Layer  
263 distortions in LU2b in cores GFS11-D and -E could be related to slumping, possibly explaining  
264 the erosional upper boundary and low thickness of LU2 in GFS11-~LUs 4 and 5 showed high-

265 frequency facies shifts in cores GFS11-C to -E (and weakly developed in core GFS11-AB). These  
266 shifts were either between carbonate muds and sandy layers (GFS11-C) or between carbonate  
267 and organic muds (GFS11-D, -E, Figs 3, S1). A single organic mud layer in core GFS11-C-LU4  
268 and a massive 10 cm thick organic mud in GFS11-D-LU4a correlate with the 9 cm thick  
269 carbonate mud of LU2 in shallow core GFS11-AB (Fig. 3). A distinction between lower and  
270 upper deposits (with the boundary between LU3 and LU4) was supported by subfossil  
271 *Cladocera* assemblages (the first DCA axis site scores showed a trend related to sediment  
272 depth; Fig. S1B).

273

#### 274 *Chronology*

275 The initiation of lake formation was dated to ~13300 cal. a BP using remains of *Arctostaphylos*  
276 *uva-ursi* and *Juniperus communis* found at 365 cm sediment depth at the lacustrine sediment  
277 base of core GFS11-~The Allerød age was confirmed by two further dates above the same  
278 layer in core GFS11-AB (Poz-61454, Poz-61452, LU5, ~12 800 cal. a BP, Tab. 2). Hence, Lake  
279 Fürstenseer See originates from melting dead-ice blocks as suggested by macrofossil remains  
280 and C/N-ratios (Słowiński 2010), similar to other lakes in the central European lowlands (Kaiser  
281 *et al.* 2012).

282 The 9 cm thick littoral carbonate muds of GFS11-AB-LU2 had minimum and maximum  
283 ages of 4730 and 5300 cal. a BP, respectively (Tab. 3). The short core GFS10-8 records the last  
284 500 years, whereas the long cores GFS11-D and -E contained sediments older than  $8945 \pm 290$   
285 and  $4307 \pm 212$  cal. a BP, respectively ( $2\sigma$ -error, lowermost samples, lake sediment base not  
286 reached, Tab. 3). Ages in all cores were in stratigraphic order, except for two too young  
287 samples in cores GFS11-D and -E suggesting contamination during core recovery (Poz-55889,  
288 Poz-61462, not considered further; Tab. 3, Fig. 4).

289 As cores GFS11-AB and -C contained several sand layers and distinct boundaries  
290 indicating hiatuses and cores GFS10-8 and GFS11-E were rather short, a detailed age-depth-  
291 model was only calculated for core GFS11-D (Fig. 4). Major sediment facies shifts had ages of  
292  $6350 \pm 130$  cal. a BP (base of LU4),  $3750 \pm 100$  cal. a BP (base of LU3),  $800 \pm 70$  cal. a BP (base of  
293 LU2) and  $220 \pm 80$  cal. a BP (base of LU1; ages and errors rounded). Sedimentation rates in core  
294 GFS11-D were highest in the upper part of the core, especially in LU2 ( $\sim 2.3 \text{ mm a}^{-1}$ ,  $\sim 220$ -800  
295 cal. a BP) and lowest in LU5 ( $\sim 0.4 \text{ mm a}^{-1}$ ,  $\sim 6400$ -9000 cal. a BP; Fig. 4), due to soft mud  
296 compaction. If the LU5 sedimentation rate is considered to be constant throughout LU5, then

297 the basal age of LU5 can be linearly extrapolated, indicating a further facies shift at  $\sim 9670 \pm 290$   
298 cal. a BP (base of LU5, Fig. 4).

299 The age-depth model was confirmed by dates from other cores and correlative LUs (Figs  
300 3A, 4, Tab. 2). For example, the base of LU3 in GFS11-E was also dated to  $\sim 3800$  cal. a BP in  
301 accordance with an age of  $\sim 3200$  cal. a BP in the lower part of GFS11-C-LU3. Tab. 3 summarizes  
302 the facies descriptions of the LUs and their estimated time of deposition based on discrete  
303 dating, the detailed age model of GFS11-D and core correlation.

304

### 305 **Interpretation and discussions**

#### 306 *Proxy interpretation in terms of lake level*

307 *Absolute lake level reconstructions from changes in sediment limit.* The determination of the  
308 modern sediment limit at 14 m w.d. from the acoustic reflections (Fig. 2) was supported by  
309 the composition of the topmost facies above and below (sandy LU1 of GFS11-AB *versus* muddy  
310 LU1-3 of cores GFS11-C, -D, -E). The presence of fine-grained carbonate muds in 10 m w.d.  
311 (GFS11-AB-LU2) indicates that even on slopes as steep as 22% fine sediment was preserved,  
312 which is much steeper than previously suggested (Håkanson & Jansson 1983; Dearing 1997).  
313 The mud deposition at  $\sim 5000$  cal. a BP, required the sediment limit and corresponding storm  
314 wave base and lake level to rise by at least 4 m. This would be higher than the 3 m Medieval  
315 lake high-stand recorded in onshore palaeosol sediment sequences (Kaiser *et al.* 2014b). Lake  
316 volume and area would have increased by at least 390 and 310% (Fig. 5). These are minimum  
317 estimates due to missing bathymetries of adjacent lakes, the unknown amount of deposited  
318 lake sediments after this high-stand and undeterminable changes in surface topography due  
319 to human impact. Furthermore, DEM boundaries were exceeded.

320 In contrast, the deposition of sand layers in 15.2 m w.d. (core GFS11-C) represents littoral  
321 erosion in times of a lowered sediment limit (Digerfeldt 1986; Dearing 1997; Pribyl & Shuman  
322 2014). The sands of GFS11-C-LU4/5 were deposited with a fine-grained carbonate matrix  
323 between  $\sim 3750$  and  $9670$  cal. a BP. Their absolute position at 210 to 280 cm sediment depth  
324 suggests that the sediment limit lowered to  $\sim 17.3$  to 18 m w.d., but remained above 19.8 m  
325 w.d. (i.e., no sand layers in core GFS11-D). Hence, a maximum lake level and sediment limit  
326 decline of 4 m can be assumed. The lake would have reduced to 53 and 43% of its modern  
327 area and volume (minimum estimates based on modern bathymetry) isolating the sub-basins  
328 (Fig. 5).

329  
330 *Relative lake level reconstruction from facies variations represented by Ca-record.* At ~5000  
331 cal. a BP, when carbonate muds were deposited in 10 m w.d., blackish organic muds  
332 accumulated at the deeper positions (tentatively in core GFS11-C-LU4 with poor age control;  
333 better resolved in core GFS11-D-LU4a; Fig. 3). This opposing pattern of carbonate preservation  
334 was probably related to carbonate dissolution in profundal regions due to stratification  
335 (Anderson *et al.* 2005), with the thermocline depth being located between the core sites AB  
336 and C.

337 High organic matter deposition and low carbonate preservation at the deep sites are  
338 associated with high lake levels for two additional reasons. First, an up to 4 m higher lake  
339 would have inundated a large area of primarily flat vegetated terrain (Fig. 5). A high amount  
340 of biomass would have degraded in the littoral zone and been winnowed towards deeper  
341 areas. Carbonate that still precipitated in the littoral and/or pelagic zone would have been  
342 more easily dissolved within a larger water volume and/or by the pH-reduction due to the  
343 extra organic acids in the water column (Håkanson & Jansson 1983; Dean 1999). Second, the  
344 supersaturation of Ca needed for carbonate precipitation would have required a much larger  
345 amount of Ca in a larger, more slowly warming water column than in a small, rapidly warming  
346 lake (Kelts & Hsü 1975; Dean 1999). For these reasons, low carbonate and high organic matter  
347 contents have generally been associated with high lake levels and cool, humid climate, e.g. in  
348 North American lakes (Anderson *et al.* 2005; Pompeani *et al.* 2012) or in Argentina (Haberzettl  
349 *et al.* 2005; Ohlendorf *et al.* 2013). This seems to be also a likely interpretation for  
350 groundwater-fed lakes of the central European lowlands.

351 Along the same line, a shallow lake favors higher rates of carbonate accumulation.  
352 Supersaturation and thresholds for carbonate precipitation is more easily reached in a rapidly  
353 warming shallow water column with increased authigenic productivity (Kelts & Hsü 1975;  
354 Dean 1999). Hence, high Ca contents that occur in LU4/5 and LU2 of the deeper cores GFS11-  
355 C, -D and -E point to lower lake levels.

356  
357 *Constraints for Ca-interpretation as palaeohydrological proxy.* Some sensitivity constraints  
358 should be considered when interpreting the Ca record as a lake level proxy in this oligotrophic  
359 lake. First, the preservation of the littoral carbonate muds in GFS11-AB that formed under a 4  
360 m higher lake level at ~5000 cal. a BP could indicate the maximum extent of the lake (Fig. 5).

361 Alternatively, it could have been just a very high lake stand that could have occurred several  
362 times to a similar extent, but one whose sediments survived intense reworking at this steep  
363 slope to preserve the record. From the sedimentary evidence alone, it cannot be judged  
364 whether other similarly low Ca-phases represent similarly high lake stands.

365 Second, the black homogenous organic muds of the topmost sediments (LU1) below  
366 the modern sediment limit indicate that i) the deposition of organic muds already occurs at  
367 lake stands similar to those of today and ii) that the instrumentally-observed lake level range  
368 of 1.3 m cannot be traced in the modern lake sediments.

369 Third, after a long period of strong fluctuations in the early and mid-Holocene down to  
370 4 m below modern lake level, Ca remained low for ~3000 years after ~3800 cal. a BP (LU3).  
371 This suggested a generally higher lake level. However, stronger fluctuations, as reported from  
372 nearby lakes (Lorenz 2007), were no longer recorded. One reason might be that thresholds for  
373 Ca-preservation were not reached, either because the lake was too high or lake level  
374 fluctuations in this time were too low to leave an imprint in the sediments. Another reason  
375 could be a reduced Ca availability in the groundwater. Bicarbonate primarily originates from  
376 local glacial deposits and was ubiquitous after the melt down of the Pleistocene ice sheets,  
377 but was reduced in the later stages of the Holocene (as evidenced by low concentrations in  
378 modern groundwater, H. Wilke, pers. comm. 2015).

379 Fourth, a rise in trophic conditions after ~800 cal. a BP, especially during Medieval  
380 times, was evidenced by the relative increase in eutrophy-tolerant subfossil *Cladocera* species  
381 in calcareous LU2 of the GFS11-C to -E cores (e.g. *Chydorus sphaericus*; Vijverberg & Boersma  
382 1997) that grouped along the first DCA axis (Fig. S1B). Higher trophic would increase algae  
383 growth and related carbonate precipitation (Kelts & Hsü 1975; Dean 1999). Establishment of  
384 human settlements and forest pasture (*sensu* Segerström & Emanuelsson 2002) in the  
385 catchment might have increased nutrient input to the lake causing a renewed higher  
386 sensitivity of the carbonate system to lake level changes. Also, stronger lake level fluctuations,  
387 which allowed the Ca-preservation-threshold to be crossed, could have been provoked by  
388 humans manipulating the local hydrological system, e.g. by drainage measures (Kaiser *et al.*  
389 2014b). In contrast, a lack of a trophic-related forcing of carbonate precipitation before 3800  
390 cal. a BP was evidenced by subfossil *Cladocera* species preferring rather oligotrophic  
391 conditions (e.g. *Rynhotalona falcata*, Bjerring *et al.* 2009) in calcareous LU4/5 of cores GFS11-  
392 C, -D and -E and GFS11-AB-LU2.

393 In summary, the Ca record reflects “relative” lake level changes with a high sensitivity  
394 of the carbonate system to fluctuating lake levels during the early to mid-Holocene (high-  
395 frequency shifts in LU4/5) and during the period of major human impact (LU2). The proxy was  
396 less sensitive during deposition of the late Holocene organic muds (LU3, LU1).

397 Additional classical palaeohydrological proxies related to the Digerfeldt approach were of  
398 limited use at this “non-classical” site (e.g. loss-on-ignition residuals as proxy for minerogenic  
399 matter was biased by high amounts of diatoms in the sediments). Common water depth  
400 sensitive macrofossils and subfossil *Cladocera* (Hannon & Gaillard 1997; Korhola *et al.* 2000)  
401 were lacking in the sediments, because of the depth and steepness of the core transect  
402 throughout the Holocene and/or the high degree of organic matter degradation. Although the  
403 second DCA axis of subfossil *Cladocera* showed a relation to modern core position (i.e.,  
404 distance to shore; Fig. S1B; highest site scores in the carbonate muds of GFS11-AB-LU2, not  
405 shown), it rather represents a habitat association (e.g. *Alonella exigua* strongly connected with  
406 macrophytes versus *Leydigia acathocercoides* and *Leydigia leydigi* living on the sediment;  
407 Bjerring *et al.* 2009).

408

#### 409 *Temporal evolution of the lake and regional comparison*

410 With the mechanisms and constraints in mind, the temporal evolution of Lake Fürstenseer See  
411 lake levels can, on the one hand, be directly affected by climate, with cooler and/or wetter  
412 periods leading to a higher water availability and more effective groundwater recharge  
413 because of lower evapotranspiration and vice versa (e.g. Anderson *et al.* 2005). On the other  
414 hand, regional vegetation composition as determinable from pollen analyses strongly  
415 influences groundwater recharge and, hence, lake levels. Deciduous tree stands (e.g. *Fagus*  
416 and *Quercus*) allow a comparably high groundwater recharge due to high stemflows and  
417 throughfall (esp. in winter), whereas conifers (e.g. *Pinus*) have a rather negative effect on the  
418 local water budget due to high evapotranspiration throughout the year (e.g. Nathkin *et al.*  
419 2012; Guswa & Spence 2012).

420 The Holocene evolution of Lake Fürstenseer See is compared to European-wide  
421 palaeohydrological records of different quality and temporal resolution. For comparability,  
422 and if not provided in the original publications, <sup>14</sup>C ages of all records were calibrated with  
423 IntCal13 (Reimer *et al.* 2013) to cal. a BP.

424

425 >9700 cal. a BP. The deposition of massive organic muds in LU6 (Fig. 4) suggests a rather high  
426 lake level during the Early Holocene. During a warming climate, organic matter was distributed  
427 and deposited in a large lake by an active lake circulation driven by long fetches and carbonate  
428 preservation was inhibited. Forests were still sparse and light with dominance of *Pinus*, *Betula*  
429 and *Corylus* (Jahns 2007; Lampe *et al.* 2009; Feurdean *et al.* 2014). Similar lake high-stands  
430 were observed in Poland at 11 300-10 500 and 9900-9500 cal. a BP (Pazdur *et al.* 1994;  
431 Michczynska *et al.* 2013). High lake levels occurred also in Switzerland and eastern France  
432 (11250-11050, 10300-10 000 cal. a BP, Magny 2004; 10 400-9000 cal. a BP, Magny *et al.* 2011),  
433 whereas in southern Sweden lake levels reached a minimum at ~10 500 cal. a BP (Digerfeldt  
434 1988; Fig. 6). Pollen-based climate reconstructions suggested rather dry conditions  
435 throughout Europe 12 000 to 9000 years ago (Mauri *et al.* 2015), and some German lakes  
436 showed lake regressions during this time (Kleinmann *et al.* 2000). However, at Lake  
437 Fürstenseer See, rather than humidity or evapotranspiration as drivers, local melting of  
438 Younger Dryas permafrost remains and dead-ice could have contributed to groundwater  
439 recharge and high lake levels (Pazdur *et al.* 1994; Lorenz 2007; Błaszczewicz *et al.* 2015).

440  
441 9700 - 6400 cal. a BP. Between ~9700 and ~6400 cal. a BP the lake was generally low and  
442 fluctuating with a few episodes of higher lake stands occurring at ~9600-9500, ~7800 and  
443 ~6800 cal. a BP as recorded by finely laminated, carbonate-rich GFS11-D-LU5 sediments  
444 intercalated with some organic muds (Figs 3, 6). During this period, sand layers intercalated  
445 with carbonate muds at core site GFS11-C, indicating that the sediment limit was up to 4 m  
446 lower than today (Fig. 5). Calcium from glacial deposits was widely available in the  
447 groundwater, sub-basins were more isolated, and fetches were reduced. This allowed  
448 thresholds for carbonate preservation to be easily crossed, reflecting a high sensitivity of the  
449 lake system even to minor lake level fluctuations. Although the lake was lower and smaller in  
450 extent, it still was at least 3 m deeper than today because the overlying 6 m sediments at site  
451 GFS11-D were not accumulated yet. This allowed intermittent anoxic conditions to preserve  
452 the fine laminations, which were also found at nearby Lake Drewitzer See. There, similar short  
453 term high level episodes during a generally low stand were reflected by few minerogenic peaks  
454 during the same period (Lorenz 2007). High-frequency lake level variations were also observed  
455 at Lake Hämelsee, but age control needs to be improved to detect comparable high-frequency  
456 changes at other German lakes (Kleinmann *et al.* 2000). Northern Central European lakes



457 reached their Holocene water level minima (at some sites 5-7 m below the modern level)  
458 especially during the early stages of this period. Afterwards, continuously rising lake levels  
459 were proposed (Fig. 6; Pazdur *et al.* 1994; Lampe *et al.* 2009; Kaiser *et al.* 2012). In the Alps, a  
460 minimum lake level was observed at 9000-8500 cal. a BP and a series of low levels thereafter  
461 (Magny *et al.* 2011). Higher lake levels occurred 9550-9150, 8300-8050 and 7550-7250 cal. a  
462 BP (Magny 2004; Fig. 6).

463 In contrast to low lake levels in north-eastern Germany, southern Swedish and Polish  
464 palaeohydrological reconstructions revealed spatio-temporally heterogeneous, but rather  
465 high lake levels peaking ~8000 years ago (Digerfeldt 1988; Pazdur *et al.* 1996; Edvardsson *et*  
466 *al.* 2012; Fig. 6). Also pollen-based climate reconstructions suggested that Central Europe  
467 experienced its wettest period during this time period (Mauri *et al.* 2015). Hence, again a  
468 regional driver for generally low lake levels in northeastern Germany should be considered:  
469 regional pollen records indicated that forests dominated by *Pinus*, with some *Betula*, *Corylus*  
470 and *Quercus* were fully established on sandy sites (Jahns, 2007; Lampe *et al.* 2009). *Pinus*, in  
471 particular, would consume most of the available water throughout the year and affect  
472 groundwater recharge negatively (Kaiser *et al.* 2012; Guswa & Spence 2012).

473  
474 6400 - 3800 cal. a BP. Between ~6400 and ~3800 cal. a BP, several shifts from carbonate to  
475 organic muds suggest intense water level fluctuations with four periods of high stands at  
476 ~6400-6100, ~5800-5600, ~5100-4900 and ~4600-4500 cal. a BP (Fig. 6). The preservation of  
477 the littoral carbonate muds in GFS11-AB that formed under a 4-m-higher lake level at ~5000  
478 cal. a BP indicates the likely maximum extent of the lake in a short time period (Fig. 5).  
479 However, there is no local onshore evidence for such high levels during the mid-Holocene so  
480 far (Kaiser *et al.* 2014b), perhaps because only “catastrophic” high-stands that move enough  
481 sediment to create, e.g. beach ridges, can be identified in the area. Regional lakes reached  
482 their maximum extents or similar lake levels to today (Kaiser *et al.* 2012). In Poland, high lake  
483 levels were reconstructed for the periods 6500-5600, 4900-4600, and 4400-3500 cal. a BP  
484 (Gałka & Apolinarska 2014; Gałka *et al.* 2013, Fig. 6), when European-wide flooding was also  
485 observed (Macklin *et al.* 2006), within the age-uncertainties supported by high-stands of the  
486 GFS11-D-record (Fig. 6). Between ~4400 and 3800 cal. a BP, carbonate muds at site GFS11-D  
487 and slump events recorded by the fining-upwards sand layers of core GFS11-C indicate lake  
488 levels ~3 m lower than today (Fig. 6), in agreement with dry bogs in northwestern Germany

489 (Eckstein *et al.* 2009). Although western Alpine lakes had been rather low since ~6000 cal. a  
490 BP (Magny 2004), the transition to cooler and wetter conditions probably caused higher lake  
491 levels in west-central Europe (6350-5900, 6500-5200, 4850-4800, and 4150-3800 cal. a BP,  
492 Magny 2004, Fig. 6).

493 A reason for the strong lake level fluctuations visible in GFS11-D-LU4 and interpreted,  
494 for example, from southern Swedish lakes during this time (Digerfeldt 1988), might be the  
495 transition from the mid-Holocene thermal maximum towards the onset of neoglaciation. The  
496 initiation of this transition was recognized as period of rapid climate change (Mayewski *et al.*  
497 2004). However, the tendency towards generally higher lake levels might also reflect  
498 transitional change in forest composition from *Pinus* to dominance of *Quercus*, *Ulmus* and  
499 *Fagus* (Jahns 2007; Lampe *et al.* 2009), which root water directly to the ground, improving  
500 groundwater recharge (Guswa & Spence 2012).

501  
502 3800 - 800 cal. a BP. The most prominent sediment facies shift at ~3800 cal. a BP suggests an  
503 abrupt shift in lake system behavior. Low Ca values indicate that the lake level was high, at  
504 least similar to today. The organic muds were well mixed suggesting an intense lake-internal  
505 circulation across the sub-basins. No high-frequency lake level fluctuations were recorded for  
506 almost 3000 years, because the thresholds for carbonate preservation were not exceeded.

507 Within the age uncertainties, this prominent facies and lake system shift might  
508 represent a response to the global climate shift at the onset of neoglaciation (~4200 cal. a BP;  
509 Mayewski *et al.* 2004; Wanner *et al.* 2008). An associated increase in wetness since the mid-  
510 Holocene was related to a gradual decrease in northern hemisphere summer insolation and  
511 was reflected, e.g. in increased fluvial activity in Germany and Europe (Macklin *et al.* 2006;  
512 Hoffmann *et al.* 2008), and rising, but strongly fluctuating water levels in Sweden  
513 (Hammarlund *et al.* 2003; Edvardsson *et al.* 2012), in the Alps (Magny 2004), Ireland (Swindles  
514 *et al.* 2010) and Great Britain (Charman *et al.* 2006). In Poland, lake levels were high during  
515 the periods 3000-950 cal. a BP (Gałka & Apolinarska 2014), 3400-300 cal. a BP (Gałka *et al.*  
516 2014) and 2550-700 cal. a BP (Gałka *et al.* 2013; Fig. 6).

517 A prominent shift in forest composition in northern central Europe (i.e. *Pinus-Quercus*  
518 forests substituted by *Carpinus* and *Fagus*) during the Early Bronze Age was probably  
519 associated with the initiation of wood extraction and forest grazing since 3800 or 3500 cal. a  
520 BP (Jahns, 2007; Ralska *et al.* 2003; Küster *et al.* 2014; Fig. 6). Hence, higher groundwater

521 recharge from increased landscape openness, stemflow and throughfall (Guswa & Spence  
522 2012) could have sustained high lake levels under a generally cooler and wetter climate.

523

524 *800 cal. a BP to present.* The lake system showed more fluctuations in carbonate deposition  
525 after ~800 cal. a BP, a time when humans started to affect the landscape more severely in  
526 multiple ways, such as changes in the drainage systems and/or the land cover, leading to  
527 locally diverse changes in the hydrological system (Jahns 2007; Kaiser *et al.* 2014b). Carbonate  
528 was accumulated, suggesting that lake levels lowered and that the lake system was again  
529 sensitive to lake level changes. This sensitivity shift may have been caused by a higher lake  
530 trophy, as subfossil *Cladocera* assemblages suggest (see above, Fig. 3E). The facies shift was  
531 accompanied by the highest sedimentation rates of the record, between ~800 and ~630 cal.  
532 a BP (LU2b-distortions, Fig. 3, 4; i.e. late Slavic and early/mid-Medieval time). The most intense  
533 human alteration of forests and drainage systems was reconstructed for the Medieval time  
534 period (~AD1290) and to a lesser extent for the 16th and 19th century, when water mills and  
535 glasswork industries were established (Küster *et al.* 2014; Fig. 6). Lake trophy at this time was  
536 rising, allowing the thresholds for carbonate preservation to be crossed again.

537 Hence, carbonate muds representing lower lake levels were preserved from the  
538 periods ~800-700 and ~500-200 cal. a BP, whereas organic muds were accumulated between  
539 ~700-500 cal. a BP. The latter is in agreement with onshore evidences that indicated a lake  
540 level rise of up to 3 m compared to today for the period AD1250-1400 (Kaiser *et al.* 2014b; Fig.  
541 6), during the onset of the cold and wet interval of the Little Ice Age (Büntgen *et al.* 2011;  
542 Wanner *et al.* 2011). Similar water level fluctuations occurred at many lakes in the region  
543 (Kaiser *et al.* 2012). In northern Polish peatlands, the period between ~650/750 and 50 cal. a  
544 BP was characterized by hydrological instability (Lamentowicz *et al.* 2009) and even drought  
545 (Marcisz *et al.* 2015). In the western Alps, in contrast, a period of high lake level was observed  
546 in 750-650 and after ~450 cal. a BP (Magny 2004), maybe related to a different circulation  
547 regime.

548 In the 18th century, the lake shifted again to dominantly organic mud deposition (LU1,  
549 Fig. 6) and the modern lake system was established. The shift coincides with a period when  
550 forest management strategies changed to conservation rather than exploitation (Messner  
551 2009), which reduced soil erosion and lake productivity and, therefore, the lake's sensitivity  
552 to record lake level changes. Vegetation changed from a rather heterogeneous structure

553 caused by the multiple ways humans used forests on a poor soil (Segerström & Emanuelsson  
554 2002) to a dominantly deciduous forest used for hunting (Messner, 2009). This may have  
555 increased groundwater recharge again and established the current level of Lake Fürstenseer  
556 See. The recent fluctuations of 1.3 m, however, did not leave an imprint in the sediments.

557

#### 558 *Multiple drivers of Holocene lake level fluctuations*

559 Commonly, records of lake level fluctuations are interpreted as evidence for climatic changes.  
560 However, additional local and regional factors can superimpose climatic effects and  
561 complicate interpretation of such records. At Lake Fürstenseer See, a major driver for the early  
562 Holocene lake high stand until ~9700 cal. a BP was the final melting of local remains of dead-  
563 ice and permafrost, which formed during the Younger Dryas (Pazdur *et al.* 1994; Błaszkiwicz,  
564 2002; Kaiser 2004; Błaszkiwicz *et al.* 2015). The locally high water availability, as evidenced  
565 by massive organic muds, might have delayed the subsequent early- to mid-Holocene low  
566 levels (3 to 4 m below modern, ~9700-6400 cal. a BP; evidenced by sand and carbonate  
567 deposition). Early Holocene lake low stands were also observed regionally (Kaiser *et al.* 2012)  
568 suggesting a response to the establishment of *Pinus* forests on sandy substrates starting at  
569 ~11 200 cal. a BP (Theuerkauf *et al.* 2014). *Pinus* contribute negatively to groundwater  
570 recharge due to their high evapotranspiration (e.g. Guswa & Spence 2012).

571 During the course of the Holocene, a general trend of rising lake levels was observed  
572 at Lake Fürstenseer See and other northeastern German lakes (Kaiser *et al.* 2012). This reflects  
573 the water level response to both: i) insolation-driven changes to a cooler and wetter mid to  
574 late Holocene climate (Magny 2004; Wanner *et al.* 2008) and ii) a gradual transition of  
575 vegetation towards the dominance of tree species (e.g. *Fagus*, *Quercus*, Ralska *et al.* 2003;  
576 Jahns 2007) that favoured higher groundwater recharge (Guswa & Spence 2012).

577 Until ~3800 cal. a BP, the GFS11 records showed additional multi-decadal to  
578 centennial-scale sediment facies changes representing water level fluctuations within the  
579 range of ~8 m. These might reflect superimposed short-term changes of moisture availability  
580 (Digerfeldt, 1988; Pazdur *et al.* 1994), which was suggested as main driver for high-frequency  
581 western European palaeohydrological changes in the few studies that compiled several  
582 regional water level records (Magny 2004; Charman *et al.* 2006; Swindles *et al.* 2010). These  
583 studies linked the position and strength of the moisture-providing westerly storm track to  
584 solar variation and North Atlantic atmospheric circulation.

585           After a ~3000 year long high-stand period of low sediment sensitivity to further lake  
586 level fluctuations, strong human impact that altered the local drainage system and land cover  
587 interacted with climate and vegetation effects in driving lake level fluctuations (*Kaiser et al.*  
588 *2012; Michczynska et al. 2013; Kaiser et al. 2014b*).

589           Hence, Holocene lake level changes were driven by several causes acting at different time-  
590 scales. Local causes influencing groundwater recharge such as melting of permafrost remains  
591 and vegetation composition interacted with long and short term climatic changes. In addition  
592 to catchment-specific processes, regional climatic and eco-hydrological feedbacks,  
593 multifaceted human impact also played an important role in driving local to regional water  
594 budgets, particularly since Medieval times. To better disentangle the involved drivers at  
595 various temporal scales, much more highly-resolved palaeohydrological archives and proxies  
596 need to be investigated and compiled following *Magny (2004)* and *Charman et al. (2006)*.

597

## 598 **Conclusions**

599           At a northeastern German lake with complex basin morphology, the combined approach of  
600 determining modern and past sediment limits from acoustic sub-bottom profiling and  
601 sediment facies along a transect of sediment cores allowed an effective estimation of the  
602 absolute lake level amplitude and relative fluctuations during the Holocene, even in a steep  
603 and deep sub-basin. The variability of carbonate preservation in the sediments (represented  
604 by the Ca record) is interpreted as a proxy for relative lake level changes with high Ca contents  
605 representing smaller than modern lake extents. However, this proxy relation was not stable  
606 through time. Sensitivity for recording lake level changes in the sediments seemed to depend  
607 on either the intensity of lake level fluctuations, the mean lake level upon which high-  
608 frequency fluctuations occur and/or the abundance of Ca in the groundwater system. Hence,  
609 the fluctuations during the instrumental period were not recorded within the lake sediments.

610           The lake was strongly fluctuating at a level 3 to 4 m lower than today during the early and  
611 mid-Holocene. Shifts of up to 4 m higher lake stands occurred during the late mid-Holocene.  
612 These extremes represent a total natural water level amplitude of 8 m. This clearly exceeded  
613 the modern range of 1.3 m lake level fluctuations during the last 40 years and occurred during  
614 a time when human impact on the lake and catchment hydrology was negligible. These strong  
615 fluctuations might be the result of differential groundwater recharge from feedbacks between  
616 vegetation composition and variable climatic background conditions. Further intense

617 fluctuations with up to 3 m higher lake levels happened during the late Holocene, when  
 618 humans diversely affected the drainage system, forest structure and lake trophy. If current  
 619 forest and water management intends to reach quasi-natural conditions within the Müritzer  
 620 national park, the long Holocene record suggests that i) future lake water level changes could  
 621 exceed the so-far-observed amplitudes and variability and ii) the hydrological response to  
 622 climate change strongly depends on forest and vegetation composition.

623  
 624 *Acknowledgements.* All technicians and the coring team of GFZ-section 5.2 that assisted in the  
 625 field and lab (G. Arnold, D. Berger, B. Brademann, F. Ott, D. Richter, R. Schedel) are  
 626 acknowledged as well as P. Dulski for help with the  $\mu$ -XRF analyses, J. Dreibrodt, N. Dräger, U.  
 627 Kienel and K. Kaiser for discussion. Two anonymous reviewers and the editor Jan A. Piotrowski  
 628 helped to improve the manuscript. K. Cook kindly checked the English of the revised text. This  
 629 study is a contribution to the Virtual Institute of Integrated Climate and Landscape Evolution  
 630 Analysis (ICLEA) supported by infrastructure of the Terrestrial Environmental Observatories  
 631 network (TERENO), both financed by the Helmholtz Association.

632

### 633 **References**

- 634 Allen, M. R. & Ingram, W. J. 2002: Constraints on future changes in climate and the hydrologic cycle. *Nature* 419,  
 635 224-232.
- 636 Anderson, L., Abbott, M. B., Finney, B. P. & Edwards, M. E. 2005: Palaeohydrology of the Southwest Yukon Territory,  
 637 Canada, based on multiproxy analyses of lake sediment cores from a depth transect. *The Holocene* 15,  
 638 1172-1183.
- 639 Birks, H.H. 2007: Plant macrofossil introduction. In Elias, S.A. (ed.): *Encyclopedia of Quaternary Science*, 2266-2288,  
 640 Elsevier, Amsterdam.
- 641 Bjerring, R., Becares, E., Declerck, S., Gross, E. M., Hansson, L.-A., Kairesalo, T., Nykänen, M., Halkiewicz, A., Kornijów,  
 642 R., Conde-Porcuna, J. M., Seferlis, M., Nóges, T., Moss, B., Amsinck, S. L., Odgaard, B. V. & Jeppesen, E.  
 643 2009: Subfossil Cladocera in relation to contemporary environmental variables in 54 Pan-European lakes.  
 644 *Freshwater Biology* 54, 2401-2417.
- 645 Błaszczewicz, M. 2002: Spätglaziale und frühholozäne Seebeckenentwicklung im östlichen Teil von Pommern  
 646 (Polen). *Greifswalder Geographische Arbeiten* 26, 11-14.
- 647 Błaszczewicz, M., Piotrowski, J. A., Brauer, A., Gierszewski, P., Kordowski, J., Kramkowski, M., Lamparski, P., Lorenz, S.,  
 648 Noryśkiewicz, A. M., Ott, F., Słowiński, M. & Tyszkowski, S. 2015: Climatic and morphological controls on  
 649 diachronous postglacial lake and river valley evolution in the area of Last Glaciation, northern Poland.  
 650 *Quaternary Science Reviews* 109, 13-27.
- 651 Brauer, A. & Casanova, J. 2001: Chronology and depositional processes of the laminated sediment record from Lac  
 652 d'Annecy, French Alps. *Journal of Paleolimnology* 25, 163-177.

- 653 Bronk Ramsey, C. 2008: Deposition models for chronological records. *Quaternary Science Reviews* 27, 42-60.
- 654 Bronk Ramsey, C. & Lee, S. 2013: Recent and planned developments of the program OxCal. *Radiocarbon* 55, 720–
- 655 730.
- 656 Büntgen, U., Tegel, W., Nicolussi, K., McCormick, M., Frank, D., Trouet, V., Kaplan, J. O., Herzig, F., Heussner, K.-U.,
- 657 Wanner, H., Luterbacher, J. & Esper, J. 2011: 2500 Years of European Climate Variability and Human
- 658 Susceptibility. *Science* 331, 578-582.
- 659 Dean, W. 1999: The carbon cycle and biogeochemical dynamics in lake sediments. *Journal of Paleolimnology* 21,
- 660 375-393.
- 661 Dearing, J. A. 1997: Sedimentary indicators of lake-level changes in the humid temperate zone: a critical review.
- 662 *Journal of Paleolimnology* 18, 1-14.
- 663 Dietze, E., Wünnemann, B., Diekmann, B., Aichner, B., Hartmann, K., Herzsuh, U., Ijmker, J., Jin, H., Kopsch, C.,
- 664 Lehmkuhl, F., Li, S., Mischke, S., Niessen, F., Opitz, S., Stauch, G. & Yang, S. 2010: Basin morphology and
- 665 seismic stratigraphy of Lake Donggi Cona, north-eastern Tibetan Plateau, China. *Quaternary International*
- 666 218, 131-142.
- 667 Dietze, E., Wünnemann, B., Hartmann, K., Diekmann, B., Jin, H., Stauch, G., Yang, S. & Lehmkuhl, F. 2013: Early to
- 668 mid-Holocene lake high-stand sediments at Lake Donggi Cona, northeastern Tibetan Plateau, China.
- 669 *Quaternary Research* 79, 325-336.
- 670 Digerfeldt, G. 1986: Studies on past lake-level fluctuations. In Berglund, B. (ed.): *Handbook of Holocene*
- 671 *Palaeoecology and Palaeohydrology*, 127-144. John Wiley & Sons, New York.
- 672 Digerfeldt, G. 1988: Reconstruction and regional correlation of Holocene lake-level fluctuations in Lake Bysjön,
- 673 South Sweden. *Boreas* 17, 165-182.
- 674 Eckstein, J., Leuschner, H. H. & Bauerochse, A. 2011: Mid-Holocene pine woodland phases and mire development
- 675 – significance of dendroecological data from subfossil trees from northwest Germany. *Journal of*
- 676 *Vegetation Science* 22, 781-794.
- 677 Edvardsson, J., Leuschner, H. H., Linderson, H., Linderholm, H. W. & Hammarlund, D. 2012: South Swedish bog
- 678 pines as indicators of Mid-Holocene climate variability. *Dendrochronologia* 30, 93-103.
- 679 Feurdean, A., Perşoiu, A., Tanţău, I., Stevens, T., Magyari, E. K., Onac, B. P., Marković, S., Andrić, M., Connor, S.,
- 680 Fărcaş, S., Gałka, M., Gaudeny, T., Hoek, W., Kolaczek, P., Kuneš, P., Lamentowicz, M., Marinova, E.,
- 681 Michczyńska, D. J., Perşoiu, I., Płóciennik, M., Słowiński, M., Stancikaite, M., Sumegi, P., Svensson, A.,
- 682 Tămaş, T., Timar, A., Tonkov, S., Toth, M., Veski, S., Willis, K. J. & Zernitskaya, V. 2014: Climate variability
- 683 and associated vegetation response throughout Central and Eastern Europe (CEE) between 60 and 8 ka.
- 684 *Quaternary Science Reviews* 106, 206-224.
- 685 Gałka, M. & Apolinarska, K. 2014: Climate change, vegetation development, and lake level fluctuations in Lake
- 686 Purwin (NE Poland) during the last 8600 cal. a BP based on a high-resolution plant macrofossil record
- 687 and sTab. isotope data ( $\delta^{13}\text{C}$  and  $\delta^{18}\text{O}$ ). *Quaternary International* 328–329, 213-225.
- 688 Gałka, M., Miotk-Szpiganowicz, G., Goslar, T., Jęsko, M., van der Knaap, W. O. & Lamentowicz, M. 2013:
- 689 Palaeohydrology, fires and vegetation succession in the southern Baltic during the last 7500 years
- 690 reconstructed from a raised bog based on multi-proxy data. *Palaeogeography, Palaeoclimatology,*
- 691 *Palaeoecology* 370, 209-221.

- 692 Gałka, M., Tobolski, K., Zawisza, E. & Goslar, T. 2014: Postglacial history of vegetation, human activity and lake-  
693 level changes at Jezioro Linówek in northeast Poland, based on multi-proxy data. *Vegetation History and*  
694 *Archaeobotany* 23, 123-152.
- 695 Germer, S., Kaiser, K., Bens, O. & Hüttl, R.F. 2011: Water balance changes and responses of ecosystems and society  
696 in the Berlin–Brandenburg region—a review. *Erde* 142, 65–95.
- 697 Gilbert, R. 2003: Spatially irregular sedimentation in a small, morphologically complex lake: implications for  
698 paleoenvironmental studies. *Journal of Paleolimnology* 29, 209-220.
- 699 Grimm, E. 1987: CONISS: a FORTRAN 77 program for stratigraphically constrained cluster analysis by the method  
700 of incremental sum of squares. *Computers and Geosciences* 13, 13-35.
- 701 Gronewold, A. D. & Stow, A. 2014: Water loss from the Great Lakes. *Science* 343, 1084-1085.
- 702 Guswa, A. J. & Spence, M. 2012: Effect of throughfall variability on recharge: application to hemlock and deciduous  
703 forests in western Massachusetts. *Ecohydrology* 5, 563-574.
- 704 Haberzettl, T., Fey, M., Lücke, A., Maidana, N., Mayr, C., Ohlendorf, C., Schäbitz, F., Schleser, G., Wille, M. &  
705 Zolitschka, B. 2005: Climatically induced lake level changes during the last two millennia as reflected in  
706 sediments of Laguna Potrok Aike, southern Patagonia (Santa Cruz, Argentina). *Journal of Paleolimnology*  
707 33, 283-302.
- 708 Haig, H., Kingsbury, M., Laird, K., Leavitt, P., Laing, R. & Cumming, B. 2013: Assessment of drought over the past  
709 two millennia using near-shore sediment cores from a Canadian boreal lake. *Journal of Paleolimnology*  
710 50, 175-190.
- 711 Håkanson, L. & Jansson, M. 1983: *Principles of Lake Sedimentology*. 320 pp. Springer, Berlin–New York.
- 712 Hammarlund, D., Björck, S., Buchardt, B., Israelson, ~& Thomsen, ~T. 2003: Rapid hydrological changes during the  
713 Holocene revealed by stable isotope records of lacustrine carbonates from Lake Igelsjön, southern  
714 Sweden. *Quaternary Science Reviews* 22, 353-370.
- 715 Hannon, G. & Gaillard, M.-J. 1997: The plant-macrofossil record of past lake-level changes. *Journal of*  
716 *Paleolimnology* 18, 15-28.
- 717 Hill, M. O. & Gauch, H. G., Jr. 1980: Detrended correspondence analysis: An improved ordination technique.  
718 *Vegetatio* 42, 47-58.
- 719 Hoffmann, T., Lang, A. & Dikau, R. 2008: Holocene river activity: analysing <sup>14</sup>C-dated fluvial and colluvial sediments  
720 from Germany. *Quaternary Science Reviews* 27, 2031-2040.
- 721 Hutchinson, G. E. 1957: *A Treatise on Limnology, Volume 1, Part 1 - Geography and Physics of Lakes*. 1015 pp. John  
722 Wiley and Sons, New York.
- 723 Jahns, S. 2007: Palynological investigations into the Late Pleistocene and Holocene history of vegetation and  
724 settlement at the Löddigsee, Mecklenburg, Germany. *Vegetation History and Archaeobotany* 16, 157-169.
- 725 Juggins, S. 2015: *rioja: Analysis of Quaternary Science Data, R package version (0.9-5)*. [http://cran.r-](http://cran.r-project.org/package=rioja)  
726 [project.org/package=rioja](http://cran.r-project.org/package=rioja).
- 727 Kaiser, K. 2004: Geomorphic characterization of the Pleistocene - Holocene transition in Northeast Germany. *In*  
728 Terberger, T. & Eriksen, B.V. (eds.): *Hunters in a changing world*, 53-73, Verlag Marie Leidorf,  
729 Rahden/Westfalen.



- 730 Kaiser, K., Koch, P., Mauersberger, R., Stüve, P., Dreibrodt, J. & Bens, O. 2014a: Detection and attribution of lake-  
731 level dynamics in north-eastern central Europe in recent decades. *Regional Environmental Change* 14,  
732 1587-1600.
- 733 Kaiser, K., Küster, M., Fülling, A., Theuerkauf, M., Dietze, E., Graventein, H., Koch, P. J., Bens, O. & Brauer, A. 2014b:  
734 Littoral landforms and pedosedimentary sequences indicating late Holocene lake-level changes in  
735 northern central Europe — A case study from northeastern Germany. *Geomorphology* 216, 58-78.
- 736 Kaiser, K., Lorenz, S., Germer, S., Juschus, O., Küster, M., Libra, J., Bens, O. & Hüttl, R. F. 2012: Late Quaternary  
737 evolution of rivers, lakes and peatlands in northeast Germany reflecting past climatic and human impact –  
738 an overview. *E&G – Quaternary Science Journal* 61, 103-132.
- 739 Kelts, K. & Hsü, K. J. 1978: Freshwater Carbonate Sedimentation. In Lerman, A. (ed.): *Lakes*, 295-323. Springer, New  
740 York.
- 741 Kirschey, T. & Oldorff, S. 2012: Ergebnisse des „Naturkundlichen Tauchens“ 2012 im Großen Fürstenseer See im  
742 Nationalpark Müritz. *Bericht des Tauchclub Nehmitzsee e.V.*, 18 pp., Tauchclub Nehmitzsee e.V.,  
743 Neubrandenburg.
- 744 Kleinmann, A., Merkt, J. & Müller, H. 2000: Climatic lake-level changes in German lakes during the Holocene. In  
745 Negendank, J.F.W. & Brauer, A. (eds.): The record of human/climate interactions in lake sediments, 55-63,  
746 *Terra Nostra* 7.
- 747 Korhola, A., Olander, H. & Blom, T. 2000: Cladoceran and chironomid assemblages as qualitative indicators of  
748 water depth in subarctic Fennoscandian lakes. *Journal of Paleolimnology* 24, 43-54.
- 749 Küster, M., Fülling, A., Kaiser, K. & Ulrich, J. 2014: Aeolian sands and buried soils in the Mecklenburg Lake District,  
750 NE Germany: Holocene land-use history and pedo-geomorphic response. *Geomorphology* 211, 64-76.
- 751 Laird, K. R., Kingsbury, M. V., Lewis, F. M. & Cumming, B. F. 2011: Diatom-inferred depth models in 8 Canadian  
752 boreal lakes: inferred changes in the benthic:planktonic depth boundary and implications for assessment  
753 of past droughts. *Quaternary Science Reviews* 30, 1201-1217.
- 754 Lamentowicz, M., Milecka, K., Gałka, M., Cedro, A., Pawlyta, J., Piotrowska, N., Lamentowicz, Ł. & Van Der Knaap, W.  
755 O. 2009: Climate and human induced hydrological change since AD 800 in an ombrotrophic mire in  
756 Pomerania (N Poland) tracked by testate amoebae, macro-fossils, pollen and tree rings of pine. *Boreas* 38,  
757 214-229.
- 758 Lampe, R., Lorenz, S., Janke, W., Meyer, H., Küster, M., Hübener, T. & Schwarz, A. 2009: Zur Landschafts- und  
759 Gewässergeschichte der Müritz. Umweltgeschichtlich orientierte Bohrungen 2004-2006 zur  
760 Rekonstruktion der nacheiszeitlichen Entwicklung. In Nationalparkamt Müritz (ed.): *Forschung und*  
761 *Monitoring*, 92 pp. Geozon Science Media, Greifswald.
- 762 Laskar, J., Robutel, P., Joutel, F., Gastineau, M., Correia, A. ~M. & Levrard, B. 2004: A long-term numerical solution  
763 for the insolation quantities of the Earth. *A&A* 428, 261-285.
- 764 Lorenz, S. 2007: *Die spätpleistozäne und holozäne Gewässernetzentwicklung im Bereich der Pommerschen*  
765 *Haupteisrandlage Mecklenburgs*, Ph D thesis, University of Greifswald, 351 pp.
- 766 Lüthgens, ~& Böse, M. 2011: Chronology of Weichselian main ice marginal positions in north-eastern Germany.  
767 *E&G – Quaternary Science Journal* 60, 236-247.

- 768 Macklin, M. G., Benito, G., Gregory, K. J., Johnstone, E., Lewin, J., Michczyńska, D. J., Soja, R., Starkel, L. &  
769 Thorndycraft, V. R. 2006: Past hydrological events reflected in the Holocene fluvial record of Europe.  
770 *CATENA* 66, 145-154.
- 771 Magny, M. 2004: Holocene climate variability as reflected by mid-European lake-level fluctuations and its probable  
772 impact on prehistoric human settlements. *Quaternary International* 113, 65-79.
- 773 Magny, M., Bossuet, G., Ruffaldi, P., Leroux, A. & Mouthon, J. 2011: Orbital imprint on Holocene palaeohydrological  
774 variations in west-central Europe as reflected by lake-level changes at Cerin (Jura Mountains, eastern  
775 France). *Journal of Quaternary Science* 26, 171-177.
- 776 Marcisz, K., Tinner, W., Colombaroli, D., Kołaczek, P., Słowiński, M., Fiałkiewicz-Kozieł, B., Łokas, E. & Lamentowicz,  
777 M. 2015: Long-term hydrological dynamics and fire history over the last 2000 years in CE Europe  
778 reconstructed from a high-resolution peat archive. *Quaternary Science Reviews* 112, 138-152.
- 779 Mauri, A., Davis, B. A. S., Collins, P. M. & Kaplan, J. O. 2015: The climate of Europe during the Holocene: a gridded  
780 pollen-based reconstruction and its multi-proxy evaluation. *Quaternary Science Reviews* 112, 109-127.
- 781 Mayewski, P. A., Rohling, E. E., Curt Stager, J., Karlén, W. r., Maasch, K. A., David Meeker, L., Meyerson, E. A., Gasse,  
782 F., van Kreveld, S., Holmgren, K., Lee-Thorp, J., Rosqvist, G., Rack, F., Staubwasser, M., Schneider, R. R. &  
783 Steig, E. J. 2004: Holocene climate variability. *Quaternary Research* 62, 243-255.
- 784 Messner, G. 2009: *Geschichte der Müritz-Nationalparkregion*. 208 pp. Förderverein Müritz-Nationalpark e.V.,  
785 Neubrandenburg.
- 786 Meyers, P. A. & Ishiwatari, R. 1993: Lacustrine organic geochemistry—an overview of indicators of organic matter  
787 sources and diagenesis in lake sediments. *Organic Geochemistry* 20, 867-900.
- 788 Michczyńska, D. J., Starkel, L., Nalepka, D. & Pazdur, A. 2013: Hydrological changes after the last ice retreat in  
789 Northern Poland using radiocarbon dating. *Radiocarbon* 55, 1712-1723.
- 790 Natkhin, M., Steidl, J., Dietrich, O., Dannowski, R. & Lischeid, G. 2012: Differentiating between climate effects and  
791 forest growth dynamics effects on decreasing groundwater recharge in a lowland region in Northeast  
792 Germany. *Journal of Hydrology* 448-449, 245-254.
- 793 Ohlendorf, C., Fey, M., Gebhardt, C., Habertzettl, T., Lücke, A., Mayr, C., Schäbitz, F., Wille, M. & Zolitschka, B. 2013:  
794 Mechanisms of lake-level change at Laguna Potrok Aike (Argentina) – insights from hydrological balance  
795 calculations. *Quaternary Science Reviews* 71, 27-45.
- 796 Oksanen, J., Blanchet, F.G., Kindt, R., Legendre, P., Minchin, P.R., O'Hara, R.B., Simpson, G.L., Solymos, P., Henry, M.,  
797 Stevens, H. & Wagner, H. 2015: *vegan: Community Ecology Package. R package version 2.2-1*.  
798 <http://CRAN.R-project.org/package=vegan>.
- 799 Pompeani, D., Steinman, B. & Abbott, M. 2012: A sedimentary and geochemical record of water-level changes  
800 from Rantin Lake, Yukon, Canada. *Journal of Paleolimnology* 48, 147-158.
- 801 Pribyl, P. & Shuman, B. N. 2014: A computational approach to Quaternary lake-level reconstruction applied in the  
802 central Rocky Mountains, Wyoming, USA. *Quaternary Research* 82, 249-259.
- 803 Punning, J., Alliksaar, T., Terasmaa, J. & Jevrejeva, S. 2004: Recent patterns of sediment accumulation in a small  
804 closed eutrophic lake revealed by the sediment records. *Hydrobiologia* 529, 71-81.

- 805 Ralska-Jasiewiczowa, M., Nalepka, D. & Goslar, T. 2003: Some problems of forest transformation at the transition  
806 to the oligocratic/Homo sapiens phase of the Holocene interglacial in northern lowlands of central  
807 Europe. *Vegetation History and Archaeobotany* 12, 233-247.
- 808 Reimer, P. J., Bard, E., Bayliss, A., Beck, J. W., Blackwell, P. G., Bronk Ramsey, C., Buck, C. E., Cheng, H., Edwards, R. L.,  
809 Friedrich, M., Grootes, P. M., Guilderson, T. P., Haflidason, H., Hajdas, I., Hatté, C., Heaton, T. J., Hoffmann,  
810 D. L., Hogg, A. G., Hughen, K. A., Kaiser, K. F., Kromer, B., Manning, S. W., Niu, M., Reimer, R. W., Richards,  
811 D. A., Scott, E. M., Southon, J. R., Staff, R. A., Turney, C. S. M. & van der Plicht, J. 2013: IntCal13 and  
812 Marine13 Radiocarbon Age Calibration Curves 0–50,000 Years cal BP. *Radiocarbon* 55, 1869–1887.
- 813 Schnurrenberger, D., Russell, J. & Kelts, K. 2003: Classification of lacustrine sediments based on sedimentary  
814 components. *Journal of Paleolimnology* 29, 141-154.
- 815 Segerström, U. & Emanuelsson, M. 2002: Extensive forest grazing and hay-making on mires – vegetation changes  
816 in south-central Sweden due to land use since Medieval times. *Vegetation History and Archaeobotany* 11,  
817 181-190.
- 818 Sherwood, S. & Fu, Q. 2014: A drier future? *Science* 343, 737-739.
- 819 Shuman, B., Pribyl, P., Minckley, T. A. & Shinker, J. J. 2010: Rapid hydrologic shifts and prolonged droughts in  
820 Rocky Mountain headwaters during the Holocene. *Geophysical Research Letters* 37, L06701.
- 821 Słowiński, M. 2010: Macrofossil reconstruction of preboreal wetland formed on dead ice block a case study of the  
822 Borzechowo mire in East Pomerania, Poland. *Studia Quaternaria* 27, 3-10.
- 823 Słowiński, M., Błaszkiwicz, M., Brauer, A., Noryskiewicz, B., Ott, F. & Tyszkowski, S. 2015: The role of melting dead  
824 ice on landscape transformation in the early Holocene in Tuchola Pinewoods, North Poland. *Quaternary*  
825 *International* 388, 64-75.
- 826 Stüve, P. 2010: Die Wasserhaushaltssituation der letzten 40 Jahre im Raum der Neustrelitzer Kleinseenplatte. In  
827 Kaiser, K., Libra, J., Merz, B., Bens, O. & Hüttel, R.F. (eds.): *Aktuelle Probleme im Wasserhaushalt von*  
828 *Nordostdeutschland: Trends, Ursachen, Lösungen*, 206–211, *Scientific Technical Report 10*. Deutsches  
829 GeoForschungsZentrum, Potsdam.
- 830 Szeroczyńska, K. & Sarmaja-Korjonen, K., 2007: *Atlas of Subfossil Cladocera from Central and Northern Europe*. 88  
831 pp. Friends of the Lower Vistula Society, Świecie.
- 832 Templ, M., Hron, K. & Filzmoser, P. 2011: robCompositions: an R-package for robust statistical analysis of  
833 compositional data. In Pawlowsky-Glahn, V. & A. Buccianti (eds.): *Compositional Data Analysis. Theory and*  
834 *Applications*, 341-355. John Wiley & Sons, Chichester.
- 835 Theuerkauf, M., Bos, J. A. A., Jahns, S., Janke, W., Kuparinen, A., Stebich, M. & Joosten, H. 2014: Corylus expansion  
836 and persistent openness in the early Holocene vegetation of northern central Europe. *Quaternary Science*  
837 *Reviews* 90, 183-198.
- 838 Tjallingii, R., Röhl, U., Kölling, M. & Bickert, T. 2007: Influence of the water content on X-ray fluorescence core-  
839 scanning measurements in soft marine sediments. *Geochemistry, Geophysics, Geosystems* 8, doi:  
840 10.1029/2006GC001393.
- 841 Tobolski, K., 2000. *Przewodnik do oznaczania torfów i osadów jeziornych, Vademecum Geobotanicum*. 508 pp.  
842 Wydawnictwo Naukowe PWN, Warszawa.

843 Velichkevich, F.U. & Zastawniak, E. 2006: *Atlas of the Pleistocene vascular plant macrofossils of Central and Eastern*  
 844 *Europe, Part 1 - Pteridophytes and monocotyledons*. 224 pp. W. Szafer Institute of Botany, Polish  
 845 Academy of Science, Kraków.

846 Velichkevich, F.U. & Zastawniak, E. 2008: *Atlas of the Pleistocene vascular plant macrofossils of Central and Eastern*  
 847 *Europe, Part 2 - Herbaceous dicotyledons*. 224 pp., W. Szafer Institute of Botany, Polish Academy of  
 848 Science, Kraków.

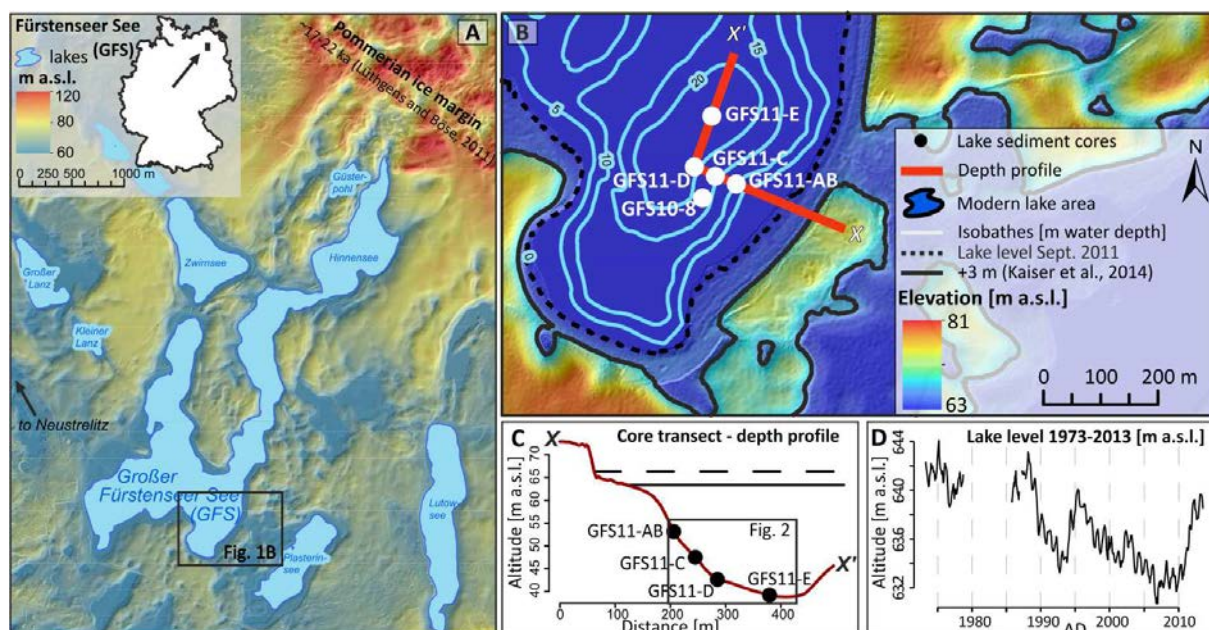
849 Vijverberg, J. & Boersma, M. 1997: Long-term dynamics of small-bodied and large-bodied cladocerans during the  
 850 eutrophication of a shallow reservoir, with special attention for *Chydorus sphaericus*. *Hydrobiologia* 360,  
 851 233-242.

852 Wanner, H., Beer, J., Bütikofer, J., Crowley, T. J., Cubasch, U., Flückiger, J., Goosse, H., Grosjean, M., Joos, F., Kaplan,  
 853 J. O., Küttel, M., Müller, S. A., Prentice, I. C., Solomina, O., Stocker, T. F., Tarasov, P., Wagner, M. &  
 854 Widmann, M. 2008: Mid- to Late Holocene climate change: an overview. *Quaternary Science Reviews* 27,  
 855 1791-1828.

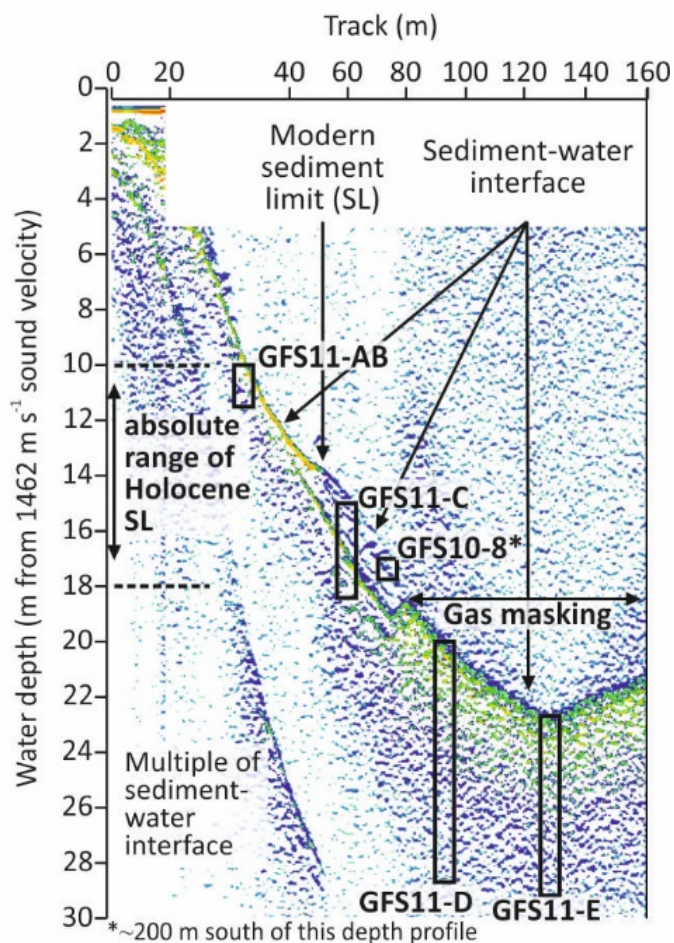
856 Weltje, G. J. & Tjallingii, R. 2008: Calibration of XRF core scanners for quantitative geochemical logging of  
 857 sediment cores: Theory and application. *Earth and Planetary Science Letters* 274, 423-438.

858

## 859 Figures

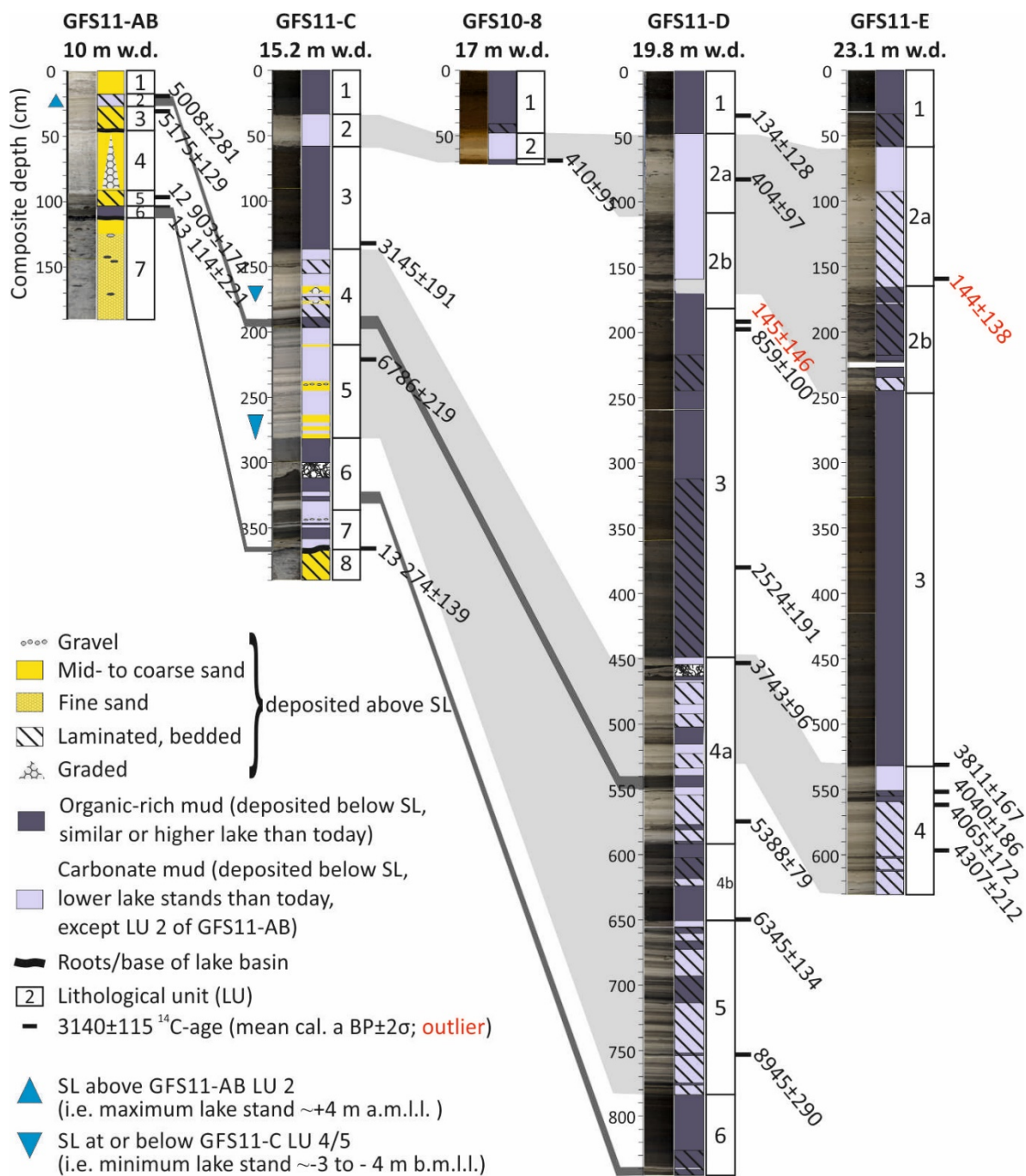


860  
 861 **Fig. 1:** A. Map of Lake Fürstenseer See within the Müritz national park, Germany. B. Location of the  
 862 sediment core transect in the southeastern bay. C. Bathymetric profile across the core transect. D.  
 863 Monthly lake level data from reading of a graduated rod for the period 1973-2013 (Stüve 2010; P.  
 864 Stüve, pers. comm. 2014).

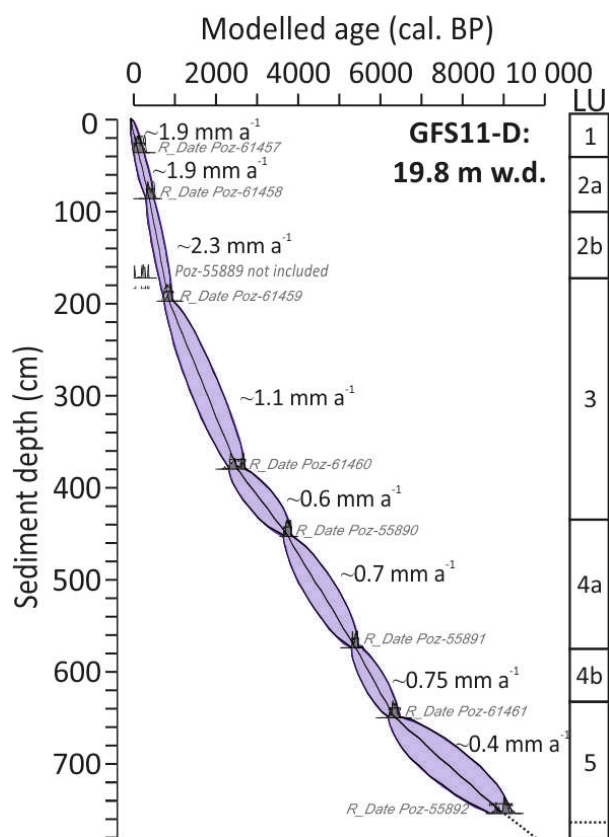


865

866 **Fig. 2:** Acoustic sub-bottom depth profile along the core transect in the southeastern bay of Lake  
 867 Fürtenseer See. Blue to green colours indicate high transparency and low impedance contrasts as  
 868 typical for water-saturated pelagic sediment, yellow to red colours indicate high backscatter from  
 869 dense, sandy sediments.



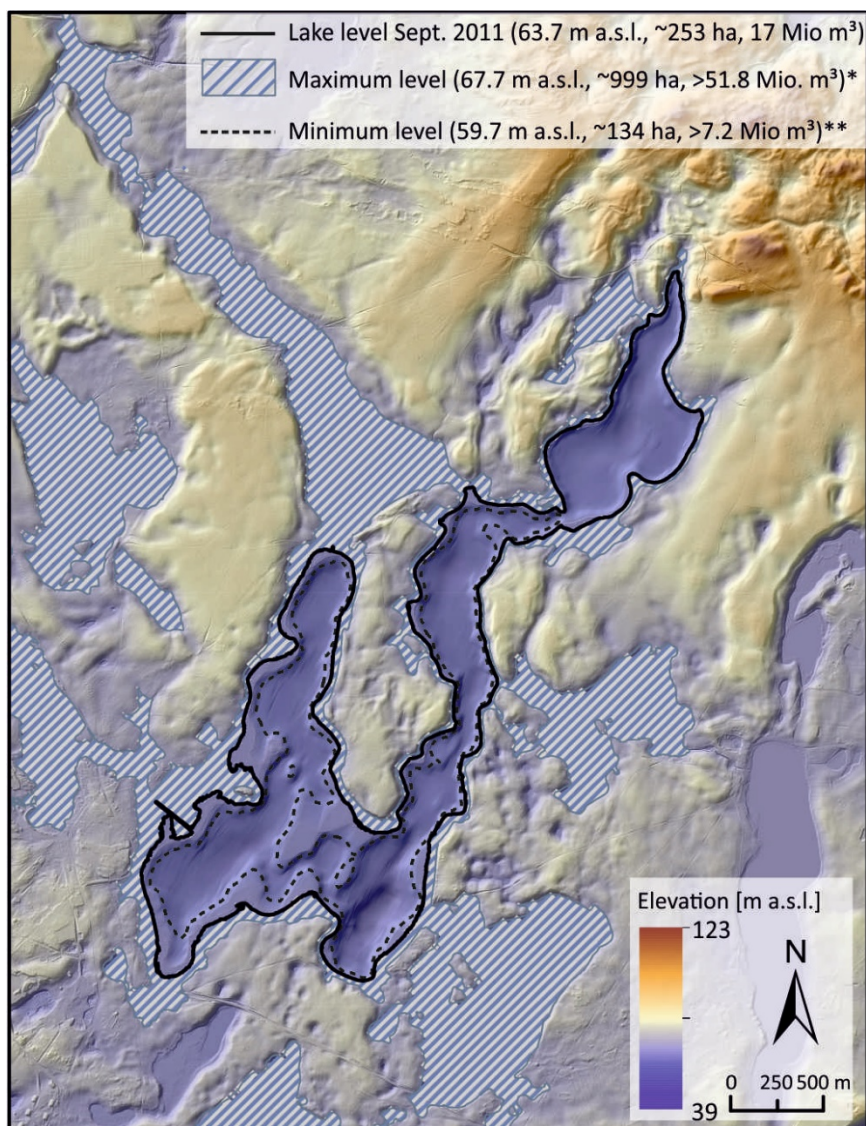
870  
871 **Fig. 3:** Correlated stratigraphies of Lake Fürstenseer See composite cores including mean dates with  
872 their 2σ-ranges (see Tab. 2). Grey bars show correlative lithological units. SL and blue triangles indicate  
873 the assumed sediment limit position.



874

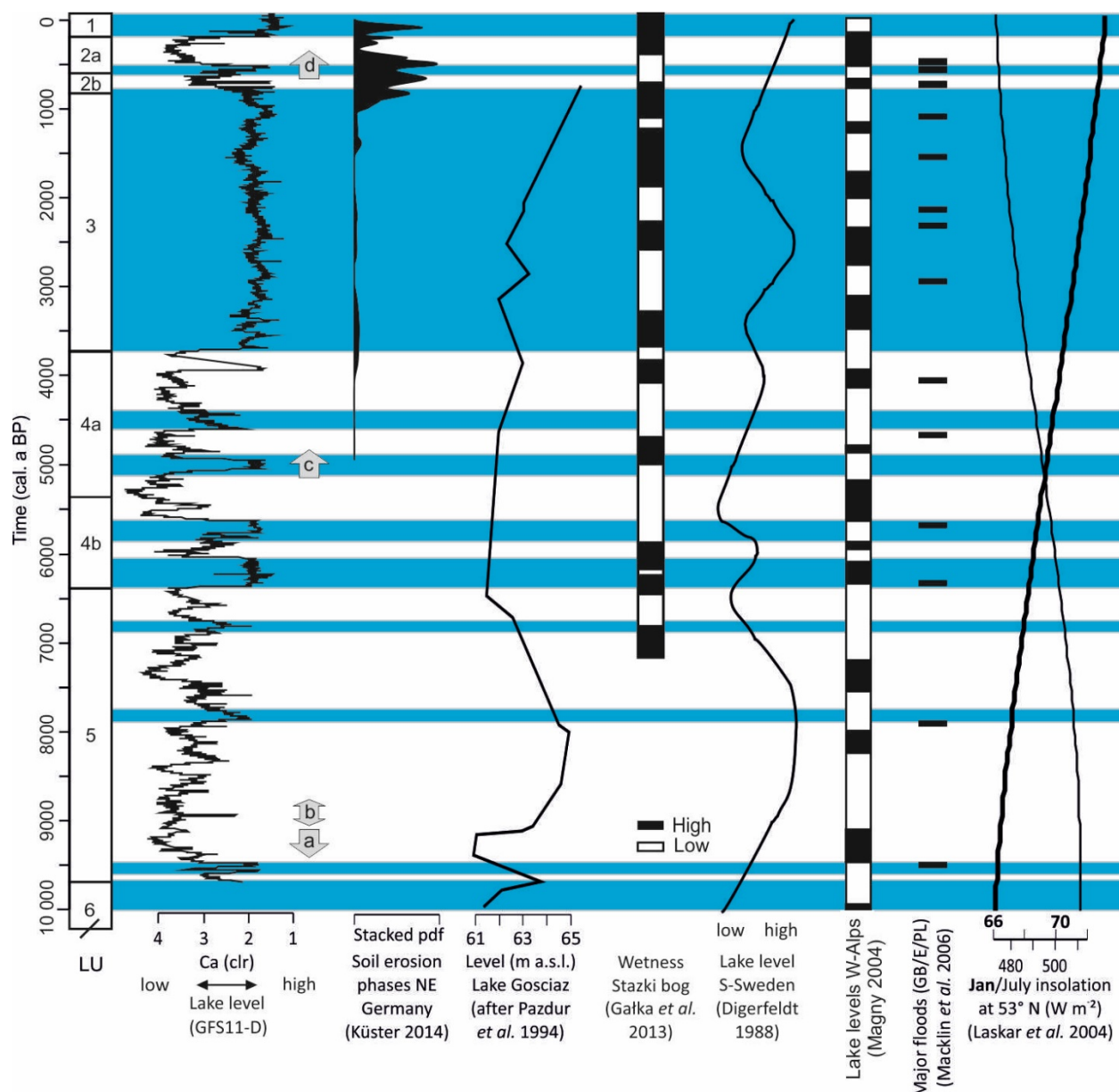
875 **Fig. 4:** Age-depth-model of core GFS11-D including sedimentation rates and lithological units (LU) for

876 comparison. Dotted line marks linear age-depth-extrapolation to base of LU5.



877  
 878 **Fig. 5:** Modern and reconstructed past extensions of Lake Füstenseer See using a bathymetric survey  
 879 (Ministerium für Landwirtschaft, Umwelt und Verbraucherschutz Mecklenburg-Vorpommern, 2013)  
 880 and an airborne laser scanning digital elevation model (Amt für Geoinformation, Vermessungs- und  
 881 Katasterwesen Mecklenburg-Vorpommern, 2013). \*minimum estimate because no bathymetric data  
 882 from adjacent lakes available, DEM boundaries exceeded and potential biases from human-induced  
 883 morphological changes. \*\*minimum estimate due to use of modern bathymetry.





884

885 **Fig. 6:** Comparison of clr-transformed Ca record (reversed axis) and lithological units (LU 1 to 6) of core  
 886 GFS11-D with regional soil erosion phases (as proxy for human impact), European proxies for wet  
 887 phases (lake levels and floodings) and seasonal insolation. a = 4 m low stand reconstructed from sand  
 888 layers in GFS11-C; b = peat in 90 cm below present lake level (Kaiser *et al.* 2014b); c = 4 m high stand  
 889 reconstructed from littoral carbonate muds in GFS11-AB; d = 3-m high-stand reconstructed by Kaiser  
 890 *et al.* (2014b). Blue bars in background indicate high-stand phases of Lake Fürstenseer See.

891

892

893 **Tables**

*Table 1.* Location of sediment cores in Lake Fürstenseer See and basinmorphometric attributes. Slope was measured using a 2 m buffer around the core location. Maximum fetch was generally from rare northerly wind directions, why a maximum fetch of the prevailing wind directions (SW to NW, P. Stüve, pers. comm. 2013) was calculated additionally.

Core name	Latitude (N) WGS84	Longitude (E) WGS84	Water depth (m)	Core length (m)	Slope (%±σ)	Distance to shore (m)	Maximum fetch (m)	Maximum fetch in prevailing wind direction (m)
GFS11-AB	13° 10' 11.6	53° 18' 2.5	10	1.9	22.5±0.8	81	1624	972 (NW)
GFS11-C	13° 10' 9.6	53° 18' 2.9	15.2	3.9	14.6±0.8	117	1594	930 (NW)
GFS11-D	13° 10' 7.6	53° 18' 3.4	19.8	8.5	8.5±1.0	156	1567	890 (NW)
GFS11-E	13° 10' 9.1	53° 18' 6.3	23.1	6.3	2.4±0.2	191	1470	1094 (WNW)
GFS10-8	13° 10' 8.42	53° 18' 1.67	17	0.7	14.9±0.1	118	1625	955 (NW)

894

895

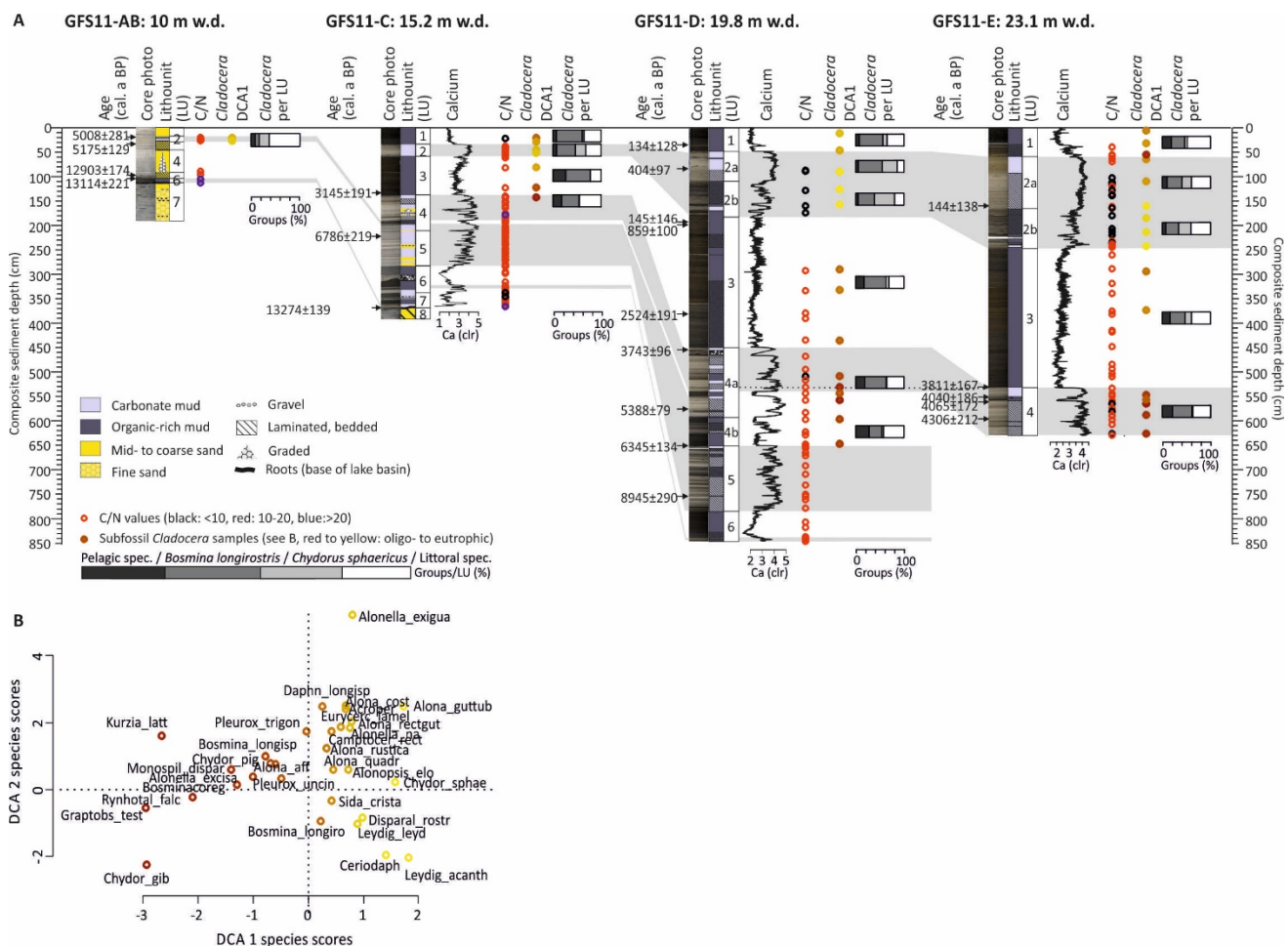
Table 2. AMS radiocarbon dates from a transect of sediment cores at Lake Fürstenseer See. Calibration of dates using INTCAL13 (Reimer *et al.* 2013) in Oxcal 4.2. Cores are sorted after water depth. Date Poz-55889 was excluded from age-depth-modelling of core GFS11-D (Fig. 4).

Core name	Lithological unit	Composite sediment depth (cm)	Represented sediment (cm <sup>3</sup> )	Material	Mean <sup>14</sup> C-age (a BP)	Error (a, 1σ)	Min. cal. age (cal. a BP, 2σ)	Max. cal. age (cal. a BP, 2σ)	Mean cal. age (cal. a BP)	Error (cal. a BP, 2σ)	Lab.Code/Reference
GFS11-A0	AB-LU2	19.25	1	<i>Pinus sylv.</i> bark	4350	80	4727	5288	5007.5	280.5	Poz-61451
GFS11-B1	AB-LU2	31.9	0.5	<i>Pinus sylv.</i> bark	4510	35	5046	5303	5174.5	129	Poz-55886
GFS11-A1	AB-LU2	97	1	<i>Larix decid.</i> cone	11040	100	12 729	13 076	12 902.5	174	Poz-61454
GFS11-A0	AB-LU2	104	1	Charcoal	11270	100	12 893	13 334	13 113.5	221	Poz-61452
GFS11-C1	C-LU3	131.15	10.5	<i>Pinus sylv.</i> bark	2960	60	2954	3335	3144.5	191	Poz-61455
GFS11-C1	C-LU5	220.8	2.3	<i>Pinus sylv.</i> bark	5960	80	6567	7005	6786	219	Poz-61456
GFS11-C2	C-LU7	365.5	0.5	<i>Arctostaphylos uva-ursi</i> seeds, <i>Pinus sylv.</i> needle, <i>Juniperus communis</i> needle	11430	60	13 135	13 413	13 274	139	Poz-55888
GFS10-8	LU2	69	0.5	plant remains	370	35	315	505	410	95	Poz-37472
GFS11-D0	D-LU1	36	1	<i>Pinus sylv.</i> bark	145	60	6	262	134	128	Poz-61457
GFS11-D1	D-LU2a	85.9	1	leaf remains	385	60	307	501	404	97	Poz-61458
GFS11-D0	D-LU3	191.7	0.5	<i>Pinus sylv.</i> needle	180	25	0	291	145.5	146	Poz-55889
GFS11-D1	D-LU3	197.2	1	Leaf remains	905	60	759	958	858.5	100	Poz-61459
GFS11-D2	D-LU3	379.7	19.5	<i>Pinus sylv.</i> bark	2365	60	2334	2715	2524.5	191	Poz-61460
GFS11-D2	D-LU4a	453	0.5	<i>Pinus sylv.</i> bark	3485	30	3647	3838	3742.5	96	Poz-55890
GFS11-D3	D-LU4a	573.8	0.5	<i>Pinus sylv.</i> bark	4645	35	5309	5466	5387.5	79	Poz-55891
GFS11-D3	D-LU4b	649.8	1	<i>Pinus sylv.</i> bark	5530	70	6212	6479	6345.5	134	Poz-61461
GFS11-D4	D-LU5	753.85	0.5	<i>Pinus sylv.</i> needle	8100	60	8655	9234	8944.5	290	Poz-55892
GFS11-E1	E-LU2a	159.4	1	<i>Pinus sylv.</i> bark	110	60	6	281	143.5	138	Poz-61462
GFS11-E3	E-LU3	531.34	1	<i>Pinus sylv.</i> bark	3535	60	3644	3978	3811	167	Poz-61464
GFS11-E3	E-LU4	552.34	1	<i>Pinus sylv.</i> bark	3685	60	3854	4225	4039.5	186	Poz-61465
GFS11-E4	E-LU4	561.76	2.3	<i>Pinus sylv.</i> bark, betula seed	3710	60	3893	4236	4064.5	172	Poz-61466
GFS11-E4	E-LU4	596.76	1	<i>Pinus sylv.</i> bark, betula seeds	3890	70	4095	4518	4306.5	212	Poz-61467

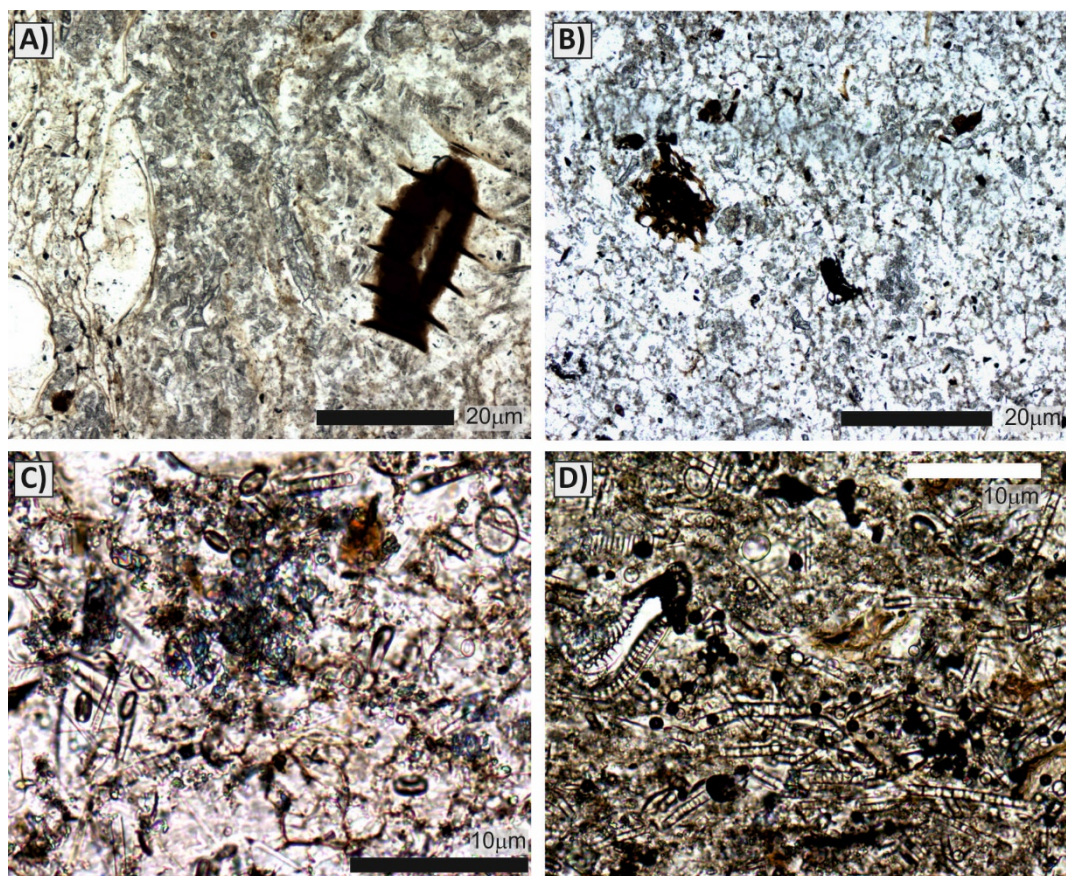
**Table 3.** Descriptions of lithological units (LU) in each core of the transect from Lake Fürstenseer See. Stratigraphy after visual descriptions (all cores), CONISS clustering using  $\square$ -XRF data of cores C, D, E as well as microscopic descriptions for cores C,D,E and AB unit 2. Chronology estimated after dates from Tab. 2 and correlation with core GFS11-D, where age-depth-model could be calculated (Fig. 4).

Core	LU	Composite depth (cm)	Description	Estimated age (maximum cal. a BP)
GFS11-AB	1	0-18	Massive medium-to-coarse sand, wavy lower boundary	modern- ~4800
	2	18-27	Laminated carbonate mud with <i>Chara spec. oogonia</i> and thin layers of amorphous organic matter, wavy lower boundary	~4800-5200
	3	27-46	Laminated coarse to fine sand with carbonatic sand layers, diffuse lower boundary	~5200-12 600
	4	46-91	Normally graded sand, distinct lower boundary	~5200-12 600
	5	91-103.4	Laminated fine sand, wavy lower boundary	~12 900-13 100
	6	103.4-110.9	Massive dark brown sandy organic mud, wavy lower boundary	~13 300
	7	>110.9	Heterogenous massive sand and gravel layers, in-situ <i>Arctostaphylos uva-ursi</i> and <i>Juniperus communis</i> roots on top	Deglaciation
GFS11-C	1	0-33.3	Blackish wet homogenous organic mud, distinct lower boundary	<300 (~AD1750)
	2	33.3-58.3	Grey carbonate mud with greyish-brown upper part, wavy lower boundary	~300 - ~900 (~AD1100)
	3	58.3-136.7	Blackish, homogenous organic mud, diffuse lower boundary	~900 - ~3800 (~1700 BC)
	4	136.7-209.8	Alternating greyish to blackish laminated carbonate mud with two normally-grading sand layers	~3800 - ~6400 (~4400 BC)
	5	209.8-281.3	Laminated carbonate muds in different shades of grey with several thin sand layers	~6400 - ~9400 (~7500 BC)
	6	281.3-336.3	Blackish massive organic mud with well-preserved lacustrine organic matter, more carbonatic in the lower part	>9400
	7	336.3-366.6	Greyish to blackish calcareous mud with layers of yellowish-amorphous gel-matrix, slightly sandy	~13 300 at the base
	8	>366.6	Heterogenous massive sand and gravel layers, in-situ <i>Arctostaphylos uva-ursi</i> and <i>Juniperus communis</i> roots on top	Deglaciation
GFS11-D	1	0-48.1	Blackish wet homogeneous organic mud, diffuse lower boundary	<300 (~AD1750)
	2a	48.1-108.9	Greyish-brown to grey finely laminated carbonate mud, diffuse lower boundary	~300 - ~630 (~AD1450)
	2b	108.9-181.9	Dark-greyish finely laminated carbonate mud with some organic-rich layers, distorted, diffuse lower boundary	~630 - ~900 (~AD1100)
	3	181.9-448.9	Blackish organic mud with faint laminations and distinct lower boundary	~900 - ~3800 (~1700 BC)
	4a	448.9-591.6	Laminations of carbonate mud in different shades of grey with layers of blackish partly massive organic mud, partly distinct boundaries	~3800 - ~5400 (~3200 BC)
	4b	591.6-650.4	Blackish organic mud with fine greyish laminae	~5400 - ~6400 (~4400 BC)
	5	650.4-782.9	Strongly alternating blackish to light-greyish laminae	~6400 - ~9670 (~7500 BC)
	6	782.9-845.4	Blackish homogenous organic mud with a thin grey carbonate layer	>9670
GFS11-E	1	0-58.3	Blackish wet homogenous organic mud	<300 (~AD1750)
	2a	58.3-164.9	Brownish-grey massive carbonate mud with faint laminations, diffuse lower boundary	~300 - ~630 (~AD1450)
	2b	164.9-247.1	Heterogenous, partly distorted, dark greyish carbonate mud with some organic-rich layers, partly finely laminated, diffuse lower boundary	~630 - ~900 (~AD1100)
	3	247.1-532.6	Blackish organic mud with faint laminations and distinct lower boundary	~900 - ~3800 (~1700 BC)
	4	532.6-630.3	Laminations of carbonate mud in different shades of grey with layers of blackish partly massive organic mud, partly distinct boundaries	~3800 - ~4500 (~2600 BC)
GFS10-08	1	0-48	Blackish homogenous organic mud, distinct lower boundary	<300 (~AD1750)
	2	48-68	Grey carbonate mud with greyish-brown upper part, wavy lower boundary to organic mud	~300 - ~470 (~AD1580)

896 Supporting Information



897  
898 **Fig. S1:** A. Transect of Lake Frstenseer See composite cores including results of μ-XRF-Ca records, C/N-  
899 ratios and subfossil *Cladocera*. Dates include their 2σ ranges (see Tab. 2). Grey bars show correlative  
900 lithological units. See legend and text for further descriptions. B. Species scores of subfossil *Cladocera*  
901 DCA with main trend along the first axis representing trophic conditions. Second axis represents  
902 proximity to water plants. Colours refer to sites scores (samples) of the first axis in the columns  
903 "*Cladocera* DCA1" in (A).



904  
 905 **Fig. S2:** Microscopic images from cores at Lake Fürtenseer See. A. Laminated carbonatic mud with few  
 906 organic remains and *Chara spec.* oogonia (GFS11-AB: ~22 cm sediment depth, LU2). B. Decomposed  
 907 organic mud with plant macro remains and little carbonate (GFS11-C: ~90 cm sediment depth, LU3).  
 908 C. Diatom-rich sediment with carbonate clumps (GFS11-E: ~75 cm sediment depth, LU2a). D. Diatom-  
 909 and organic-rich sediment with post-depositional pyrite (GFS11-E: ~555 cm sediment depth, LU4).  
 910

*Table S1.* Average values of discrete geochemical analyses sorted after cores and lithological unit (LU). SD is the respective standard deviation for at least 3 samples of the parameter to the left. Minimum and maximum values of a certain parameter were marked in bold-italics and bold, respectively. Grey bars mark blackish organic mud layers, other units were dominated by carbonate-rich muds.

LU	Dry density (g/cm <sup>3</sup> )	SD	Water content (%)	SD	TN (%)	SD	TC (%)	SD	TOC (%)	SD	TIC (%)	SD	CaCO <sub>3</sub> (%)	SD	C/N	SD
A2	0.6	0.2	61.1	7.4	0.3	0.2	13.0	3.8	4.2	2.0	<b>8.7</b>	2.8	<b>72.7</b>	23.0	12.3	0.9
C2	0.1	0.1	88.1	4.6	1.7	0.8	21.4	6.9	17.5	8.1	3.9	1.6	32.8	13.2	10.5	0.3
C3	<b>0.1</b>	0.0	<b>92.7</b>	2.5	<b>2.9</b>	0.6	<b>32.6</b>	6.2	<b>31.2</b>	5.8	1.3	1.3	11.1	10.4	11.0	0.6
C4	0.4	0.5	74.0	21.5	1.0	0.5	15.6	7.0	11.9	5.5	3.7	2.0	30.8	16.7	13.0	1.0
C5	0.6	0.2	59.3	11.1	0.4	0.3	8.6	4.8	5.8	3.1	2.8	2.5	23.5	20.7	13.7	1.5
C6	0.3	0.1	77.2	3.8	1.5	0.8	18.5	7.6	16.6	8.1	1.9	1.4	15.8	11.7	11.3	0.5
C7	<b>0.8</b>	0.4	<b>54.7</b>	14.0	<b>0.3</b>	0.1	<b>4.9</b>	1.6	<b>3.4</b>	1.2	1.5	0.9	12.6	7.6	14.0	1.4
D2a	0.2	0.0	84.5	1.3	1.1	0.1	15.4	0.3	8.8	1.4	6.5	1.8	54.5	14.7	<b>8.2</b>	1.8
D2b	0.1	0.0	90.8	1.3	2.5	0.4	25.3	3.8	24.4	3.2	0.9	1.0	7.6	8.6	9.8	0.3
D3	0.1	0.0	92.1	0.5	2.6	0.2	29.5	3.3	28.3	3.5	1.1	0.9	9.3	7.8	10.8	0.4
D4a	0.1	0.0	87.7	3.1	1.9	0.6	23.9	4.0	20.7	6.3	3.2	2.5	26.4	20.9	10.7	0.8
D4b	0.1	0.0	88.7	2.5	2.5	0.7	30.8	4.8	29.3	6.6	1.5	2.1	12.3	17.7	11.7	0.6
D5	0.2	0.0	84.8	2.6	1.8	0.4	25.6	3.1	22.2	4.6	3.5	1.7	29.1	14.4	12.1	0.6
D6	0.3	0.2	77.5	13.3	1.7	1.1	19.7	10.6	18.1	11.6	1.6	2.4	13.5	19.6	12.5	2.2
E1	0.2	0.1	90.3	0.6	1.9	0.4	21.9	1.9	20.1	3.1	1.8	1.6	15.0	13.7	10.6	1.4
E2a	0.3	0.1	85.3	2.3	1.0	0.2	14.9	2.4	10.6	2.3	4.4	2.1	36.2	17.3	10.5	2.1
E2b	0.2	0.0	86.7	2.4	1.7	0.4	20.4	3.1	16.5	3.6	3.9	2.0	32.7	16.7	9.6	1.0
E3	0.1	0.0	89.6	1.7	2.1	0.3	22.9	2.5	22.5	2.8	<b>0.4</b>	0.5	<b>3.1</b>	4.3	10.8	0.3
E4	0.2	0.0	84.4	2.8	1.5	0.5	20.3	2.8	15.3	4.1	5.0	2.8	41.3	23.4	10.2	1.7

911

*Table S2.* Mean abundances of subfossil *Cladocera* in different units of cores GFS11.

Abundances in %. Littoral species: *Acroperus harpae*, *Alona affinis*, *Alona costata*, *Alona guttata tuberculata*, *Alona quadrangularis*, *Alona rectangula/guttata*, *Alonella excisa*, *Alonella exigua*, *Alonella nana*, *Alonopsis elongata*, *Camptocercus rectirostris*, *Chydorus globosus*, *Chydorus piger*, *Eurycercus lamellatus*, *Monospilus dispar*, *Pleuroxus trigonellus*, *Pleuroxus uncinatus*, *Rynhotalona falcata*, *Sida cristallina*. Pelagic species: *Bosmina (E.) coregoni*, *Bosmina (E.) longispina*, *Daphnia longispina-group*.

Core - lithological unit	Pelagic	Littoral	Bosmina longirostris	Chydorus sphaericus	n
AB-LU2	9.0	61.8	8.3	20.8	2
C-LU1	7.2	35.2	53.6	3.9	2
C-LU2	7.7	31.5	38.7	21.9	3
C-LU3	26.5	22.2	51.3	0.0	1
C-LU4	18.1	44.9	36.2	0.7	1
D-LU1	7.6	34.6	48.8	9.1	2
D-LU2a	5.4	13.8	50.0	30.8	1
D-LU2b	5.1	19.3	34.0	41.6	2
D-LU3	17.3	30.7	45.2	6.7	3
D-LU4a	18.5	35.5	44.7	1.3	4
D-LU4b	28.0	42.1	26.3	3.7	2
E-LU1	19.8	50.8	29.5	5.9	3
E-LU2a	12.5	48.8	38.7	24.4	3
E-LU2b	10.0	54.2	35.8	33.9	3
E-LU3	18.5	45.2	36.2	15.7	2
E-LU4	21.7	37.2	41.1	2.0	5

912